Faculty of Philosophy, Sciences and Letters of Ribeirão Preto - FFCLRP

Postgraduate Program in Physics Applied to Medicine and Biology (FAMB)

University of São Paulo - USP

Quantification of Radiodermatitis through Image Processing

Quantificação de radiodermatite através do Processamento de Imagens

Supervisee: Ignacio Agustín Verdugo Naranjo

Supervisor: Prof. Dr. Juliana Fernandes Pavoni

Co-Supervisor: Prof. Dr. George Cunha Cardoso

Ribeirão Preto, Brazil – 2019.

IGNACIO AGUSTÍN VERDUGO NARANJO

Quantification of Radiodermatitis through Image Processing

Quantificação de radiodermatite através do Processamento de Imagens

Dissertation presented to Faculty of Philosophy, Sciences and Literature of the University of São Paulo, as part of the requirements for acquirement the grade of Master of Sciences. Concentration area: Applied Physics to Medicine and Biology.

Supervisor: Prof. Dr. Juliana Fernandes Pavoni
Co-Supervisor: Prof. Dr. George Cunha Cardoso

Ribeirão Preto – SP

2019

FICHA CATALOGRÁFICA

Serviço de Documentação da Universidade de São Paulo
Faculdade de Filosofia, Ciências e Letras de Ribeirão Preto

Verdugo Naranjo, Ignacio Agustín

Quantification of Radiodermatitis through Image Processing / Ignacio Agustín Verdugo Naranjo; Orientador: Prof. Dra. Juliana Fernandes Pavoni, Co-Orientador: Prof. Dr. George Cunha Cardoso. Ribeirão Preto – SP, 2019.

114 f.:il.

Dissertation (M.Sc. - Postgraduate Program in Physics to Medicine and Biology) - Faculty of Philosophy, Sciences and Literature of the University of São Paulo, 2019.

1. Radiotherapy. 2. Radiodermatitis. 3. Image Processing. 4. Skin. 5. Polarized Light.

Name: Ignacio Agustín Verdugo Naranjo

Title: Quantification of Radiodermatitis through Image Processing

Quantificação de radiodermatite através do Processamento de Imagens

Dissertation presented to Faculty of Philosophy, Sciences and Literature of the University of São Paulo, as part of the requirements for acquirement the grade of Master of Sciences.

Approved in:

Examination Board

Prof. Dr. _____

Institution: _____

Judgment: _____

Prof. Dr. _____

Institution: _____

Judgment: _____

Prof. Dr. _____

Institution: _____

Judgment: _____

ACKNOWLEDGEMENTS

First of all, I would like to thanks Dr. Juliana Pavoni for accepting me as a masters student. I recognise it must have not been easy to agree to work with a student you hardly even know, from another country, that speaks another language and that worked in a different area along his undergraduate degree. Thanks for all the patience, advices, guidance and help throughout this two years.

I am thankful to Dr. George Cardoso for being brave to go on board on a challenging project with me and Juliana, which was far outside his research area. Thanks for all your commitment and passion when explaining your ideas for this work. We definitely would not have made it without you.

My sincere thanks to all the workers in the radiotherapy unit of the *Hospital das Clinicas de Ribeirão Preto*. Secretaries, technicians, nurses, medical physicists and medical doctors. Special thanks to all medical doctors residents, Felipe, Anielle, Ana Carolina and Alexandre. Thanks for all the knowledge you shared with me, and for helping and accompany me with all the medical returns, and for the help in the evaluation of all the images. Thanks as well to Dr. Gustavo Viani, for all his help and ideas along the image acquisition.

Thanks to all the members of the DART-3D research group, Carolina, Fernanda, Pedro Henrique, Fred and Jessica. Thanks for all the advices, guidance, suggestions and talks in the laboratory in the past years.

I am also thankful to my friends made in the university along my units. Iara, Seti, Sudi, and Kleython. Your partnership helped me when I arrived to a physics department, city and country I barely knew. Thanks for all the lunch time and coffee time shared, and trips to congresses as well.

Moreover, thanks to all my friendships made here in Brazil, who helped in adapting to this new and rich cultures, Tsukamoto's and Griebeler's family. Eduardo Henrique da Costa and Denis Ribeiro, thanks for all your partnership and even more, friendship since I arrived to Brazil.

Many thanks to all my Chilean friends who supported me and hold my claims every day of the years. César, Javiera, Vania, Loreto, Cristóbal and Pablo. Thanks for standing all my infinite voice messages seeking for advices and friendship. I would have not made it without you guys. Thanks for even being so far away from home, for making me feel like I was in Santiago talking with Chilean Spanish. I am eternally grateful.

Furthermore, thanks to my Brazilian Family. Thanks to Gisele Ponich, Laura Mondadori, Lucas Clementino, Valeria Estanislau, Claudio Clementino and all your family for all the huge support you gave me since my first day in Brazil. Thanks for all your infinite help and talks. Thanks for making all the effort of understanding my "Portuguese" since I started learning it, and for accepting me as one more member of your family.

At last, thank to my family, starting with my father. Thanks for supporting the idea of me being here in Brazil, even though in the beginning it was not a good idea. Thanks to my sister, Anai. Since the day I left home I have missed you every day. Thanks to my beloved mother, for all you support and kindness this two years. Thanks for all the long calls throughout this time, that made me feel like we were just talking about anything at home, and even though we were far apart, we know we are totally connected every second. Thanks for all. At least, but not last, thanks to my fiancée, Carolina Clementino, for sharing with me every single day of my masters. For standing my sad days, my "I'm not in the mood for anything" days, and for my happy days. Thanks for letting me share with you all my mistakes and achievements. For holding on all my claims, and giving me support and partnership when I most needed. I do not regret a single day, the moment I chose to come to Brazil and be by your side. All this, all this effort is for you, for us, for our future. And well, also thanks to my beloved dogs, Djoko and Luke. I love you!

ABSTRACT

Radiodermatitis is an ionizing radiation acute reaction of the skin. The appearance of the lesion presents a red visual appearance known as erythema, caused by an increase in subpapillary vascular plexus blood volume. Erythema rating is currently done qualitatively using the "RTOG / EORTC Late Radiation Morbidity Scoring Schema." At present, there is no quantitative method to assess the degree of injury that is affecting the skin throughout Breast Cancer therapy used in the clinical setting. This study proposes a novel method using digital, polarized light images to evaluate erythema. After the approval of the Research and Ethical Committee of the University of São Paulo, 23 breast cancer patients (>18 years old) were randomly chosen with different skin colour, TUMOUR types, surgery history, treatment type, and were followed up throughout their treatments. Circularly polarized light digital images of the patients were taken along the treatment. For each visit day, eight pictures were taken in 2 different positions (frontal and lateral) in different setups. Image registration between images of different days, for the same patients, was done using anatomical regions, skins marks, and tattoos in the border of the treatment field. The ROIs chosen for RGB colour-space analysis were the ones that reached at least grade 1 during treatment. To decrease the effect flash illumination variations from day to day, image intensities were normalized by the average intensity of a white stripe added outside the treatment area near the ROI. Each erythema was independently evaluated by physicians using the RTOG schema so that it could to test and validate the image method under development. For analysis, different groups were analysed: white ,brown skin, and dark skin. All three groups included hypofractionated vs. conventional treatment. All groups included patients with radiodermatitis grade 0, 1 and 2. It was verified that the RGB normalized intensities decrease as the radiodermatitis grade increases and that brown skin presents a more pronounced decrease. The most sensitive channel to radiodermatitis grade was the green one. The most statistically significant sensitivity in the image method was found in the differentiation between radiodermatitis grade 0 and 1 for the white and brown skin patients. The present study demonstrated a novel approach to evaluate radiodermatitis quantitatively. Despite similar past attempts in the literature, they all lack in the number of patients and the diversity of patients. This work presented a simple methodology that has to be further developed as an objective radiodermatitis quantification methodology to help the physician practice.

Funding Sources

This study was financed in part by the *Coordenação de Aperfeiçonamento de Pessoal de Nível Superior – Brasil (CAPES)*- Finance Code 001.

RESUMO

A radiodermatite é uma reação aguda da radiação ionizante da pele. A aparência da lesão apresenta uma aparência visual vermelha conhecida como eritema, causada por um aumento no volume sanguíneo do plexo vascular subpapilar. Atualmente, a classificação de eritema é feita qualitativamente usando o "Esquema de pontuação de morbidade por radiação tardia do RTOG / EORTC". Atualmente, não existe um método quantitativo para avaliar o grau de lesão que está afetando a pele ao longo da terapia do Câncer de Mama usada no cenário clínico. Este estudo propõe um novo método usando imagens digitais de luz polarizada para avaliar o eritema. Após a aprovação do Comitê de Ética e Pesquisa da Universidade de São Paulo, 23 pacientes com câncer de mama (> 18 anos) foram escolhidos aleatoriamente, com diferentes tipos de pele, tipos de TUMOUR, história de cirurgia, tipo de tratamento e acompanhados durante seus tratamentos. . Imagens digitais de luz polarizada circularmente dos pacientes foram tiradas ao longo do tratamento. Para cada dia de visita, oito fotos foram tiradas em duas posições diferentes (frontal e lateral) em diferentes configurações. O registro de imagem entre imagens de diferentes dias, para os mesmos pacientes, foi feito utilizando regiões anatômicas, marcas de peles e tatuagens na borda do campo de tratamento. Os ROIs escolhidos para análise de espaço de cor RGB foram os que atingiram pelo menos o grau 1 durante o tratamento. Para diminuir as variações do efeito flash de iluminação do dia para dia, as intensidades de imagem foram normalizadas pela intensidade média de uma faixa branca adicionada fora da área de tratamento perto da ROI. Cada eritema foi avaliado independentemente por médicos usando o esquema RTOG para testar e validar o método de imagem em desenvolvimento. Para análise, foram analisados diferentes grupos: branco, pele morena e pele escura. Todos os três grupos incluíram tratamento hipofracionado vs. convencional. Todos os grupos incluíram pacientes com radiodermatite grau 0, 1 e 2. Verificou-se que as intensidades normalizadas RGB diminuem à medida que o grau de radiodermatite aumenta e a pele morena apresenta uma diminuição mais acentuada. O canal mais sensível ao grau de radiodermatite foi o verde. A sensibilidade estatisticamente mais significativa no método de imagem foi encontrada na diferenciação entre radiodermatite grau 0 e 1 para os pacientes de pele branca e parda. O presente estudo demonstrou uma nova abordagem para avaliar quantitativamente a radiodermatite. Apesar de tentativas anteriores semelhantes na literatura, todas elas carecem do número de pacientes e da diversidade de pacientes. Este trabalho apresentou uma

metodologia simples que deve ser desenvolvida como metodologia objetiva de quantificação de radiodermatites para auxiliar a prática do médico.

Fontes de Financiamento

Este estudo foi financiado em parte pela Coordenação de Aperfeiçoamento de Pessoal de Nível Superior (CAPES) - Código Financeiro 001.

Table of Contents

LIST OF FIGURES

LIST OF TABLES

Introduction

1.1 Introduction

Radiotherapy is one approach used for the treatment of cancer. It can be used for any part of the body since the use of radiation helps to eliminate or reduce TUMOURs without having to operate the patient. The target of this technique is the DNA, where the radiation leads to failure of mitosis and cell death [1] . Over the course of the treatment, the skin (which is the first layer of body tissue to receive the radiation) will receive more or fewer doses of radiation according to the type of treatment employed [2]**,** and will suffer damage because of its radiosensitivity. Some studies suggest that up to 95% of breast cancer patients treated with radiotherapy will experience cutaneous reaction [1], [2].

There are two types of skin side effects: acute and late. The acute effect has a visual appearance in which the skin begins to turn red throughout the treatment. This colour, better known as erythema, is caused by an increase in blood volume in the subpapillary vascular plexus [3] . The extent of erythema will depend on the dose, field size, fractionation and beam quality within an effort to diminish the damage to the skin [1].

At present, different tools are used to assist a physician with this assessment. The Radiation Therapy Oncology Group (RTOG) and the European Organisation for Research and Treatment of Cancer (EORTC), presented in 1995 a research-based method for the validation of skin assessment, which is a Scoring Schema for skin which goes from grade 0 (no skin damage) to 4 (ulceration bleeding and necrosis), and where grade 5 relates to the death of the patient associated with radiation late effects (**Table 1-** RTOG / EORTC Late Radiation Morbidity Scoring Schema for skin, where grade 5 is death directly related to radiation late effects. (*https://www.rtog.org/ResearchAssociates/AdverseEventReporting/RTOGEORTCLateRadiationMorbidityScoringSchema.aspx*)) [4]. Also, another method used in radiation therapy treatment planning is the Fitzpatrick Scale (**Figure 1**) [5], where clinical staff can inform how likely it is for the patients to develop acute skin reactions depending on their type of skin.

Table 1- RTOG / EORTC Late Radiation Morbidity Scoring Schema for skin, where grade 5 is death directly related to radiation late effects. (*https://www.rtog.org/ResearchAssociates/AdverseEventReporting/RTOGEORTCLateRadiationMorbidityScoringSchema.aspx*)

Organ Tissue	0	Grade 1	Grade 2	Grade 3	Grade 4	Grade 5
Skin	None	Slight Atrophy, Pigmentation change, Some hair loss	Patch atrophy, Total hair loss	Marked atrophy, Gross telangiectasia	Ulceration	Death directly related to radiation late effects

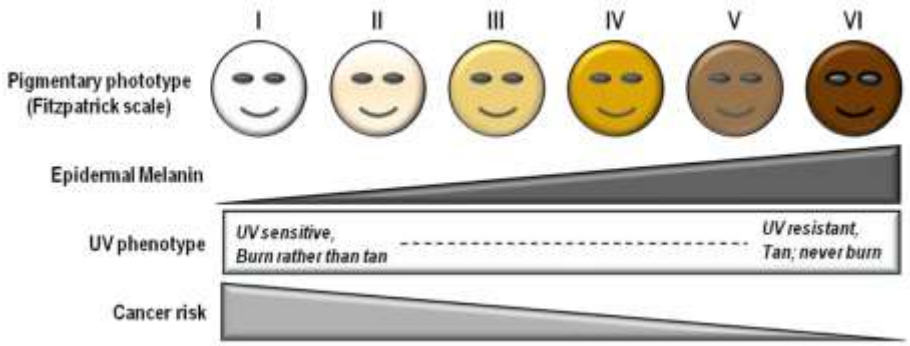

Figure 1 - Fitzpatrick Scale (J.D., 1995) [6]

However, the evaluation methods mentioned above are based on the visual inspection and may be subject to inter-observer variability. Quantitative methods for this erythema evaluation have been studied such as optical assessments [7], [8], [9] and imaging-based assessments using ultrasound [10], magnetic resonance [11] or digital colour photography [12],[13]**,** but all of them presents a limitation and the gold standard method to evaluate radiodermatitis is still the visual inspection. Considering radiodermatitis specifically, few studies have been published trying to propose a metric for it in the last 20 years, being the most relevant ones described below.

One of the first studies is from Mattsson et al (1996). This study was a novel using digital image analysis, that is a non-invasive technique that allows one to get a reproducible and quantitative analysis of radiodermatitis. They obtained images at 30 minutes, 1 hour, 2 hours, 4 hours and 12 hours post thermal burn for 12 different volunteers. Later, the images were analyzed in two colour systems, RGB (Red, Green and Blue) and HSI (Hue, Saturation and Intensity), and the intensities analyses showed a pronounced erythema the first hour, a decrease for the next hours except for the last one, where the intensity increased [14].

Another early study is by Wengström *et al* (2004) [15]. Motivated by the subjective and qualitative method of visual assessment for skin reactions, they evaluated two ways of objectively measure, validate and compare skin lesions, using reflectance spectrometry and digital images. They worked with 53 breast cancer patient treated with 6MV photon beams who undergone breast-conservative-surgery. Their therapy was delivered five days a week, with 2 Gray (Gy) per fractions up to 50Gy. The skin area of the breast was divided into five sections: axilla, areola, medial breast, lateral breast and inframammary fold. Oncology nurses visually and individually assessed the patients at 0, 24 and 50 Gy, in the treatment position and with a normal indoor lightning in the treatment room. Their findings for the digital imaging method for all the 53 patients showed that for the five different sections, there was a decrease in the pixel intensity (*Figure 2)*. Thus, the pixels getting darker shows that indeed the region is getting darker as well. Differences in each section shows that there are areas with different sensitivities to radiation.

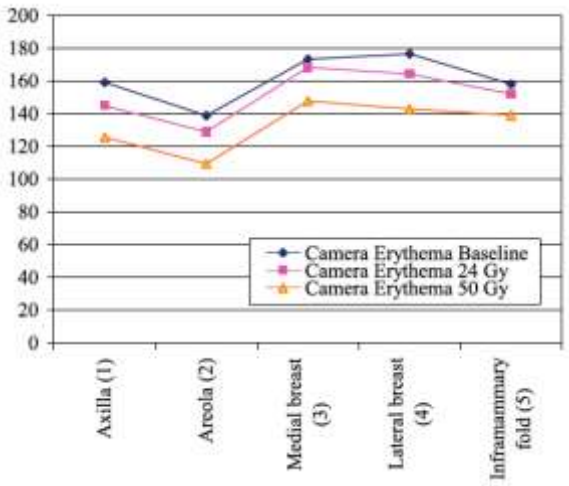

Figure 2– Mean values for the 53 patients in Wengström et al research [15] .

In 2007, Yamamoto *et al* proposed a methodology for quantification of erythema and pigmentation based on theories of the multilayered skin model, obtaining an erythema index (EI) and melanin index (MI), derived by processing RGB images of the skin. Based on Lambert-Beer Law, the absorbance of the skin at a wavelength λ (A_λ), is

$$A_\lambda = \log(1/R_\lambda) = M_\lambda C_m + H_\lambda C_h + D \quad (1.1)$$

where A_λ is the reflectance at λ, M_λ and H_λ are the coefficients dependent on the absorbance spectra of melanin and haemoglobin, and C_m and C_h represent the amounts of melanin and haemoglobin in the melanin and blood layers, and D is the pseudo absorbance of the dermis constant along the wavelength of visible light. Assuming two wavelengths, λ_1 and λ_2 , and A_1, A_2, M_1, M_2, H_1, H_2, for absorbance and coefficient values at λ_1 and λ_2. So the difference between A_1 and A_2 is

$$A_1 - A_2 = (M_1 - M_2)C_m + (H_1 - H_2)C_h \quad (1.2)$$

Choosing λ_1 and λ_2 so that M_1 - M_2 is nearly zero will make (Eq. 1.2) a linear function, so the Parameter A1-A2 is suitable for an erythema index (EI). For the EI, it was chosen λ_1 for the green band, and λ_2 for the red band, so considering R as the ratio of the brightness of each channel (R,G,B), to the brightness of a white reference in the image field,

$$A_1 - A_2 = \log(1/R_{\text{green}}) - \log(1/R_{\text{red}}) \quad (1.3)$$

Four different digital cameras were used besides a white piece of paper placed right next to the ROI. The authors tested their results with In vitro examinations using different concentrations of haemoglobin and melanin solutions; and with clinical patients trying to quantify skin test reaction, granulation tissue and extraction of blood vessels. In their results, linearity between EI, MI and haemoglobin and melanin concentration agreed with the expected results. For UV-induced erythema and pigmentation, they obtained an acceptable linear correlation. The only requirement for obtaining this good results as stated by the authors, is obtaining the images under constant and consistent conditions, this because the index values depends on the camera used as well as distance from objects and illumination.

In 2008, Nyström *et al*, besides testing digital imaging as an assessment method, tried Laser Doppler Imaging and Near Infrared spectroscopy. In breast cancer patients, they measure the radiation-based erythema in 6 different intervals along treatment. Skin lotion was tested in the breast as well as, for reducing erythema and were compared to regions in the same breast without lotion. They did a follow up of 50 breast cancer patients with total mastectomy who were treated with electron therapy (2Gy/fraction, 50Gy in total). On the irradiated skin, three test sites were chosen, where 2 of them were treated with skin lotion, and the other one, without. When taking the pictures, white balance and exposure differences were corrected with a white reference. In conclusion, they could detect erythema at low radiation doses [1] .

Putora *et al*, in 2010 proposed an automated method for radiation therapy erythema quantification based on Java. They developed a program that can automatically evaluate the redness of images. First, a list of all files with a JPG ending was retrieved. Then, the files are opened and all pixel colour in the RGB colour space, independently for each channel, for the whole image are retrieved. For studying the numerical value variation of the pixels, a ratio was used:

$$ratio = \frac{2\times Red\,Value}{Green\,Value+Blue\,Value} \tag{1.4}$$

The program was tested to demonstrate the scapability of detecting a rise in erythema on human skin, with a volunteer that applied a warming lotion on this left thigh. Then, pictures were obtained every 15 seconds after application. In their results, they manage to see an increase in erythema values. In their discussion they assumed that there is a chance that in a clinical practice of their method would work [16] .

In 2013, Bourouis *et al* proposed an innovative method based on a low cost smartphones integrated camera to identify cancer. They trained a neural network for skin classification using skin datasets of normal and abnormal state (100 images of each). The input RGB images were converted in a one dimensional vector containing all the red, green and blue values. Their results give a detection rate of 96.50% [17] .

One of the recent studies is from 2015 of Matsubara *et al*, obtained images of skin erythema of 6 patients under arbitrary lighting conditions for carbon beam therapy patients 3 hours, 30

days, and 90 days after irradiation. Studying the three channels of the RGB space, they obtained a linear response between skin dose and pixel value. In this study three important further analyses were mentioned. First, imaging with a fixed light condition is necessary to obtain precise data (e.g. obtaining images in a darkened room). Second, as only the skin colour of Japanese people was studied which presents small colour variabilities between the population, a study with other types of skins would give more information. Moreover, at last, they used carbon ion radiotherapy patients and assumed that a similar analysis could be applied to data from photon or proton beam therapy [18].

In 2016, *Carrara et al* published a correspondence comment on Matsubara's work. They discuss on one of their hypothesis, which says that the degree of skin erythema could be calculated from skin dose. Carrara also implemented a quantitative method for skin erythema. measurements due to photon radiotherapy in breast patients. Using reflectance spectrophotometry, they obtained images of 61 patients treated with 6/15 MV in a treatment of 50Gy (2Gy/fraction). They calculated with a superposition algorithm, the average dose $<D_{fold}>$ to a small volume of the inframammary fold. The skin reflectance measurements were done in the same place the $<D_{fold}>$ was calculated before the treatment began and every 6 fractions till the end. Radiation oncologists assessed the skin using the RTOG scoring system. Their results showed, based on a high sample of patients (61 vs 6 of Matsubara *et al*), that there is no linear relationship between RBA and $<D_{fold}>$. RBA is a linear fit equation that considers the clinical evaluation of the physicians [19] .

In 2016, a novel method was proposed by Madooei *et al*[20], to evaluate the effectiveness of hyperspectral images (HSI) for assessment of skin reactions in radiotherapy. In comparison to reflectance spectroscopy and imaging photography, hyperspectral imaging has the advantage of being able to provide a spatial and spectral representation of an affected area. An hyperspectral camera can divide the spectrum into thin image slices than can reveal spectral structures that may not be detected to the eye, or even to a RGB camera.

As a pilot study, they did not use actual cancer patients. They worked with healthy volunteers in a controlled experiment. A ROI was selected in form of a rectangular area inside the forearm of the volunteer (*Figure 3).* HSI and RGB values were obtained, and a baseline image of the ROI was taken before inducing an erythema, which was induced by a plastic bar striking the

skin for 3 minutes until the skin would become red. After this, the ROI was imaged again with both techniques

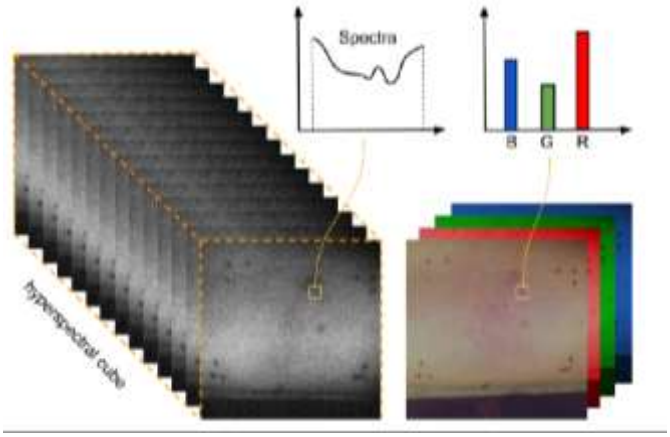

Figure 3 – Hyperspectral ROIs for a single RGB image. [20]

For their clinical assessment, they proposed a new scoring system, as seen in *Figure 4*, for their experiment to assess the intermediate stages of skin reactions. During the experiment, a physician would score erythema of the ROI. After, the physician annotated RGB images by contouring erythema areas and assigning erythema scores.

Condition	Score	Description
Very faint erythema	1	Appears as a slight increase in redness (very light pink) of the skin from baseline.
Faint erythema	2	Skin reaction is more apparent. Borders are more clearly defined.
Bright erythema	3	Erythema is clearly apparent, skin is bright pink and borders clearly defined.
Very bright erythema	4	Erythema is clearly apparent, skin is bright red and borders clearly defined.

Figure 4 – New Scoring system proposed for radiation erythema

Their results for three healthy volunteers showed that different classes of erythema can be linearly separable in the hyperspectral domain, and that the spectral information beyond visible spectrum is useful for skin erythema assessment.

A well-stablished method to study biological tissue uses linearly polarized light, as the propagation of light through biological tissues causes photon polarization changes due to scattering of tissues. That is why images with polarized light can distinguish the light that reflects from the tissue surface, from the light that enters deep into the tissue before finnaly escaping as diffuse reflectance and whose state of polarization has been completely [3]**.** Thus,

it is possible to distinguish this superficially retro-dispersed light from the fully reflected diffused light which is dominated by light penetrating deep into the dermis.

A study by Steven L. Jacques, "Imaging skin pathology with polarized light" [3] summarizes techniques prior to the year 2002, and also shows a technique that uses a polarized light imaging to at the moment of taking an image, it provides rich image details of subepithelial tissue.

The Jacques technique [3] is able to obtain images within a depth of 300 μm. A glass plate comes in contact with the skin and is optically coupled to the skin by a drop of water. The camera only collects light that has entered the skin and is back-scattered towards the camera. The acquisition of the image with the camera polarizer oriented parallel to the illuminator polarization accepts subsurface brightness. Acquiring a second image with the polarizer oriented perpendicular to the illuminator mainly accepts deeply scattered photons. Finally, an algebraic combinations of the two images produces an images display either the outer surface of the skin of the sub-epithelial region (100 μm to 300 μm depth) (*Figure 5***)**. This type of analysis has not been applied to radiodermatitis and considering the ability to observe skin damage at a depth where the human eye is not able to perceive, radiodermatitis in patients could be discovered before the erythema fully develops. This knowledge could be helpful in planning a patient's treatment.

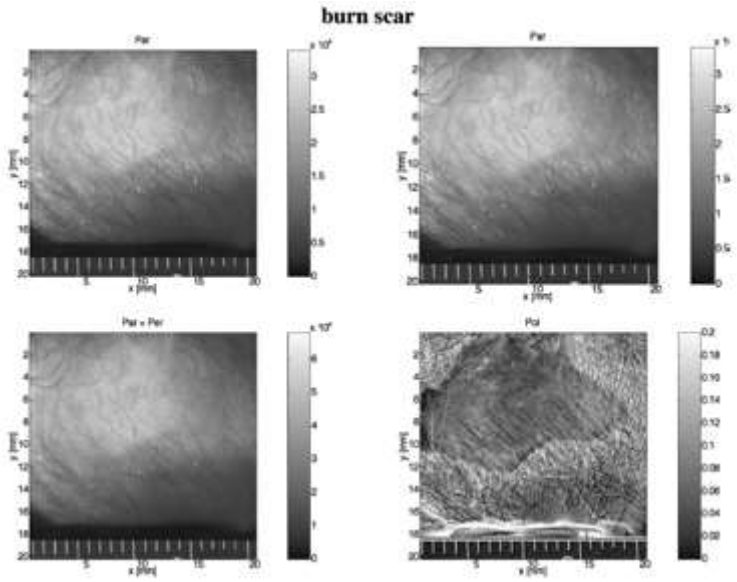

Figure 5 - Images of a normal skin imaged with a polarized filter. The image on the superior left size was obtained with the filter parallel to the illumination, the superior right image was obtained with the polarizer perpendicular to the illumination. The inferior left image is a sum

of both perpendicular and parallel image. At last the inferior right one is the Polarized image. The Polarized image suppresses the superficial scatter revealing the superficial structural of the skin [3].

This study aims to present a simple metric of the skin erythema evaluation by using digital colour photography acquired using polarized light for white and brown skin colours that could be used to help physicians to eliminate the subjectivity of the visual evaluation. The main advantage of this technique is the possibility of achieving information of the skin surface and underneath layers, which is possible because the propagation of light through biological tissues causes loss of photon polarization due to scattering in the tissues. This way, images with polarized light can distinguish the light that reflects back from the surface tissue from the light that deepens into the tissue fabric before finally escaping as diffuse reflectance and whose state of polarization has been completely randomized [3]. Thus, it is possible to distinguish this superficially retro-reflected light from the fully reflected diffused light which is dominated by light penetrating deep into the dermis.

The present study is organized as follows. We first present a summarized theoretical framework explaining the imaging, light polarization, radiation therapy and skin parts of the research. Then the methodology of the image acquisition and image processing is presented. Next, the results for patient image analysis, followed by a discussion and at last the conclusions. Also, the appendix A is the consent term the patients had to sign before being part of the research, and in the appendix B the research article of this work.

Theoretical Framework

2.1 Image Acquisition

Images are a combination of an illumination source and, either a reflection or absorption, of the energy of the elements of the scenery we want to image . Depending on the nature of the source, illumination energy is reflected from, or transmitted through, objects. When reflected of transmitted energy is focused onto a photoconverter, energy is converted into visible light.

Digital cameras use sensors for image acquisition. For example, in *Figure 6* we can see three different sensor arrangements used to transform illumination energy into digital images.

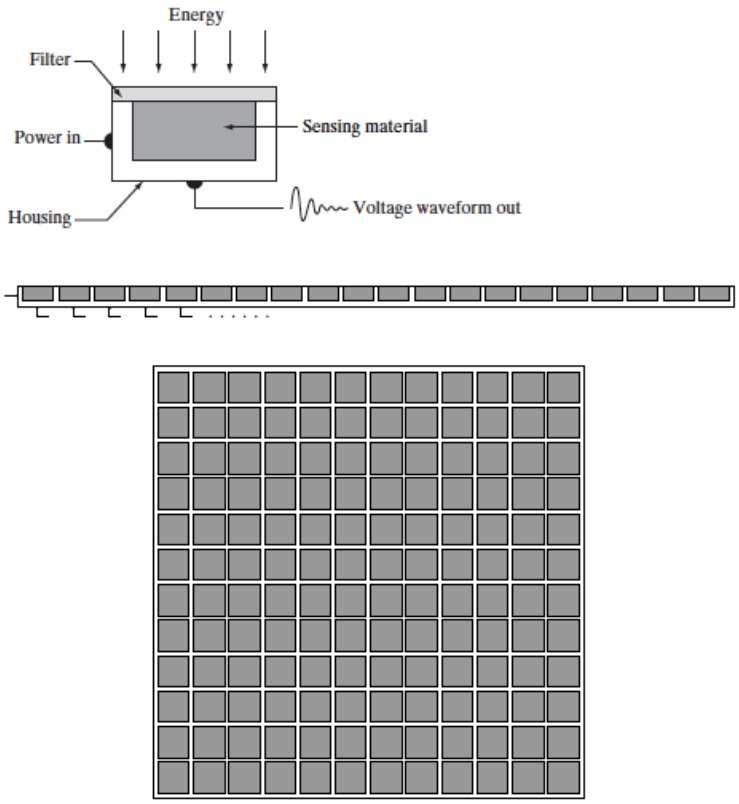

Figure 6 – Different types of sensor arrangements [21].

First, there is a single imaging sensor. Then a line sensor, and at last an array sensor. Both three are capable of transforming incoming energy into a voltage by the combination of input electrical power and sensor material that is responsive depending on the type of energy that is being detected. The output voltage waveform is digitally quantized from each sensor [21].

2.1.2 Image Acquisition using Sensor Arrays

The main arrangement found in digital cameras nowadays are a typical individual sensor arranged in a 2-D array, better known as CCD array. The response in each sensor of this type of array is proportional to the integral of the light energy projected toward the surface of the sensor [21].

The main way array sensors works requires illumination source energy being reflected in a scene element. Then, the imaging system collects the incoming energy and focus it onto an internal image plane. Commonly the illumination is light, so the front end of the imaging system is a lens which will project the scene onto the lens focal plane. Then, the sensor array will produce outputs proportional to the integral of the light received at each sensor (*Figure 7*).

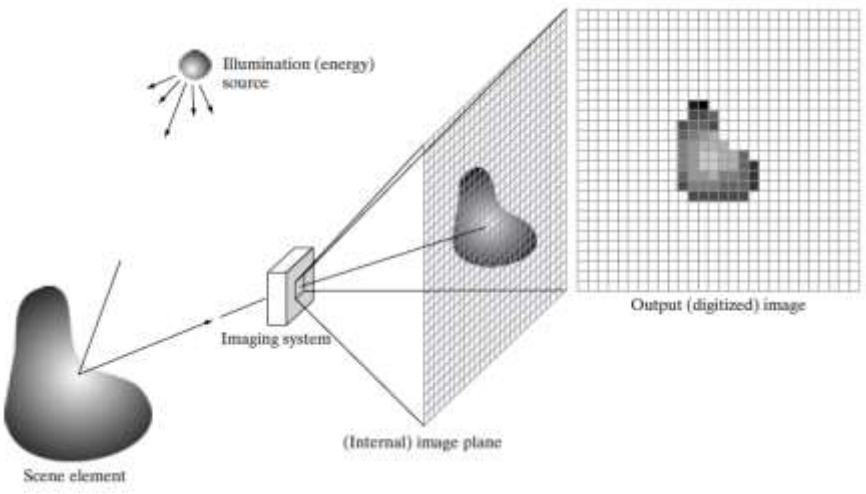

Figure 7 – Example of the digital image acquisition process [21].

2.2 Image Processing

2.2.1 Colour

The colours that humans perceive in an objective are determined by the nature of the light reflected from the object, as visible light is composed by a narrow band of frequencies in the electromagnetic spectrum. For example, green objects reflect light with the wavelengths in the 500 to 570 nm range while absorbing most of the energy of the other wavelengths.

Inside the eyes we have about 6 to 7 million sensors responsible for colour vision known as cones that can be divided into three principal sensing categories (red, green and blue). As seen in *Figure 8*, approximately 65% of all cones are sensitive to red light, 33% to green light, and only about 2% to blue.

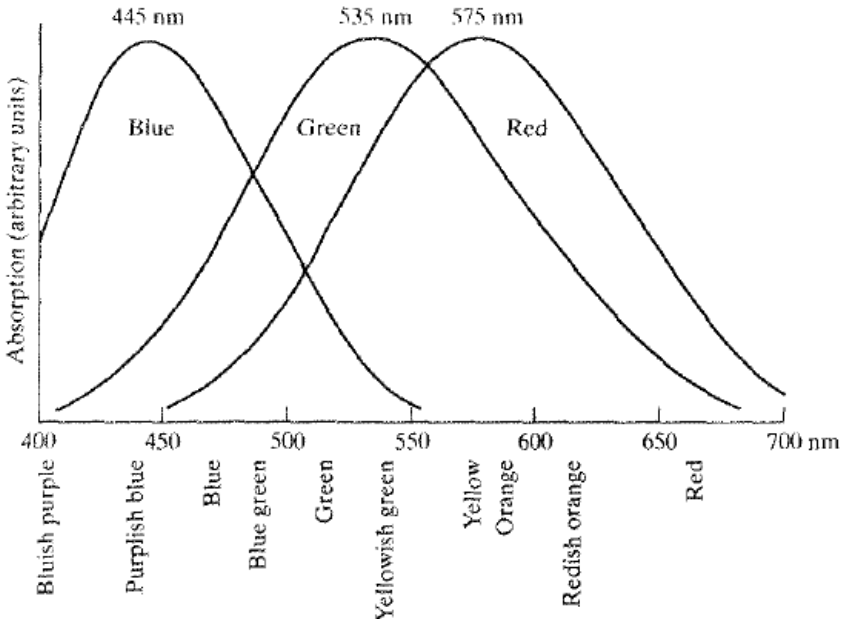

Figure 8 - Absorption of the light by the red, green and blue cones in the human eye **[21].**

2.2.2 Colour Spaces

Colour Models (or colour spaces) are used for the represent colour by a single point in an specific coordinate system and subsystem. For digital image processing, the colour models are oriented toward colour monitors and printers. The most commonly used are the RGB (red, green, blue), CMY (cyan, magenta, yellow), CMYK (cyan, magenta, yellow, black), and the HSI (hue, saturation and intensity).

2.2.2.1 RGB Colour Space

In this space model base on a cartesian coordinate system, every colour appears as a combination of the components red, green, and blue as seen in *Figure 9.* In this case, the gray scale extends from black to white along the line joining these two points. The different colours can be represented as vectors extending from the origin. In this example, all colour values have been normalized son that the cube is the unit cube.

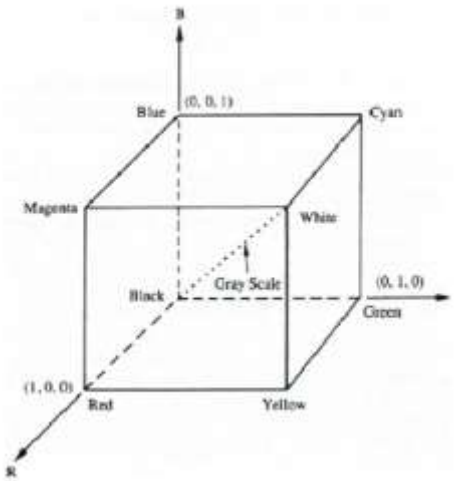

Figure 9 – RGB colour cube. Cyan, magenta and yellow are at three corners; red, green and blue appears on another three corners. Black is at the origin, and white is at the corner farthest from the origin [21].

When an image is fed into a RGB monitor, it consists of three component images which combined produce a composite colour image.

2.2.5 Geometrical Transformation

Let's consider an image *f* and a pair of pixel coordinates *(x,y).* Applying a geometric distortion to produce a new image *g* with coordinates *(x'y')*. Thus,

$$x'=r(x,y)$$

and

$$y'=s(x,y)$$

where *r(x,y)* and *s(x,y)* are the spatial transformations that produced the distorted image *g*.

Commonly, it is not possible to formulate a set of analytical functions *r(x,y)* and *s(x,y)* that describe the geometric distortion process of an image plane. So the solution is to formulate the spatial relocation of the pixels using *tiepoints*, which are a subset of pixels whose location in the input and output images is known precisely.

Considering the *Figure 10*, we can see a distorted quadrilateral region with its vertices that we will consider as tiepoints.

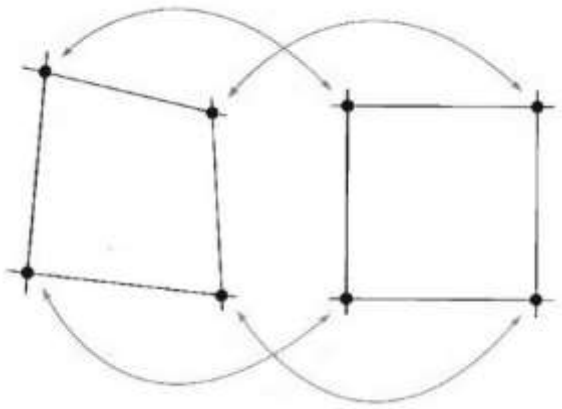

Figure 10 - Corresponding tie points in two image segments [21]

Modelling the geometric distortion by a pair of bilinear equations as follow:

$$r(x,y)=c_1x+c_2y+c_3xy+c_4 \qquad (2.1)$$

and

$$s(x,y)=c_5x+c_6y+c_7xy+c_8 \quad (2.2)$$

we obtain that

$$x'=c_1x+c_2y+c_3xy+c_4 \quad (2.3)$$

and

$$y'=c_5x+c_6y+c_7xy+c_8 \quad (2.4)$$

As seen in *Figure X*, as we have a total of eight known tiepoints, we can solve for the eight coefficients c_i, i=1,2,…,8. The coefficients constitute the geometric distortion model used to transform all pixels within the quadrilateral region defined by the tiepoints used to obtain all coefficients. The transformation described above is a type of affine transformation.

2.3 Polarization

When considering light as a transverse electromagnetic wave, the optical disturbance is the plane of vibration of the electric field (*Figure 11).* The plane of vibration of the magnetic field is ignored for optical purposes since optical resonances in materials do not posses magnetic dipole allowed transitions.

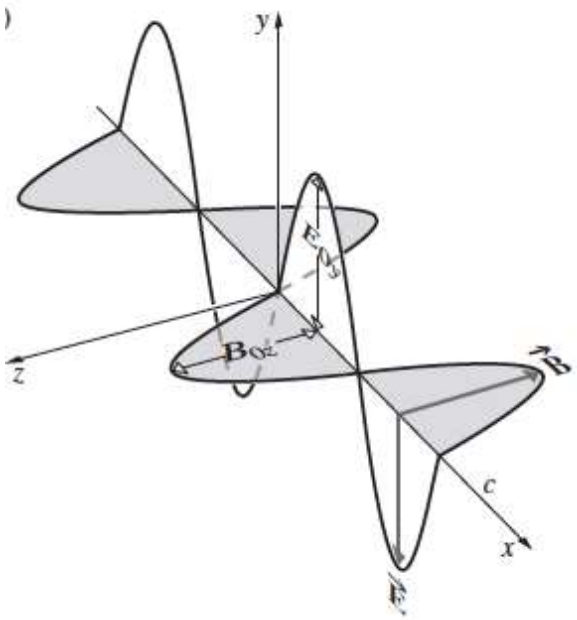

Figure 11 – Electromagnetic wave which magnitude and sign varies in time [22]**.**

Let us consider two harmonic, linearly polarized light waves with the same frequency and direction. In the case their electric field vectors are colinear, the disturbances will result in a linearly polarized wave. On the other hand, if the two light waves have their electric field directions perpendicular to each other, the resultant wave may or may not be linearly polarized. How can we observe, produce, change and make use of it? [22]

2.3.1 Linear Polarization

For a given light wave, let us consider two orthogonal optical disturbances:

$$\vec{E}_x(z,t) = \hat{\boldsymbol{\imath}} E_{0X} \cos(kz - \omega t)$$

and

$$\vec{E}_y(z,t) = \hat{\boldsymbol{\jmath}} E_{0X} \cos(kz - \omega t + \varepsilon)$$

where ε is a phase difference between the waves. The resultant disturbance is the vector sum of the waves:

$$\vec{E}(z,t) = \vec{E}_x\,(z,t) + \vec{E}_y(z,t)$$

If ε is zero or an integral multiple of ± 2π, the Eq. (2.3) becomes:

$$\vec{E} = \left(\hat{\imath}\vec{E}_{0x} + \hat{\jmath}\vec{E}_{0y}\right)\cos(kz - \omega t)$$

Thus, the resultant wave has a fixed amplitude of (**i***E*$_{0x}$+**j***E*$_{0y}$) which means as seen in *Figure Xa,* the wave is linearly polarized. As the waves advance toward a plane of observation, it can be seen a single resultant $\vec{E}$ oscillating cosinusoidally in time (*Figure 12b)* characterizing linear polarization of light.

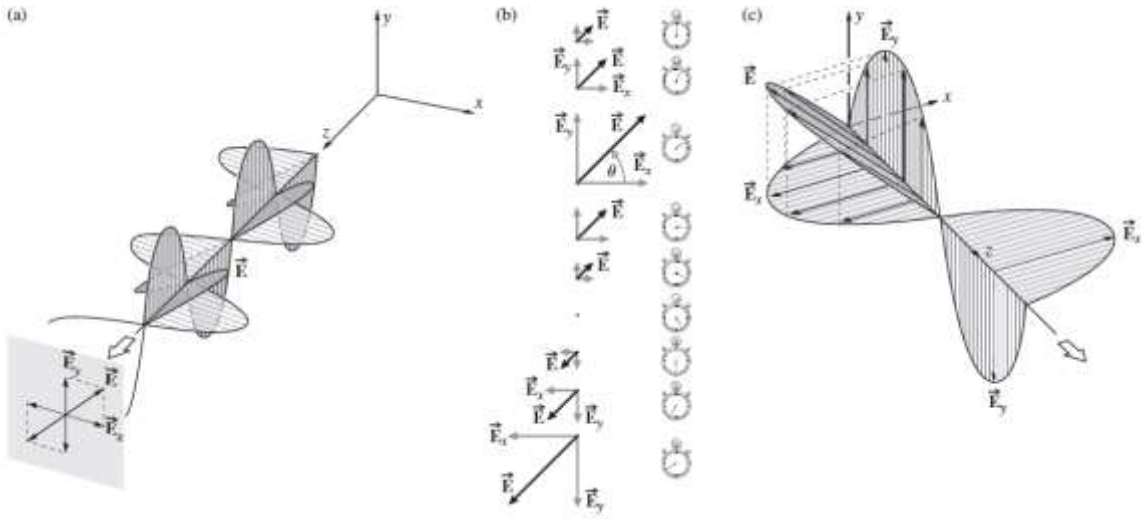

Figure 12 – Linear Light. (a) The Electric field linearly polarized in the first and third quadrants. (b) Same Oscillating field as in (a) viewed from another point. (c) Light Linearly polarized in the second and fourth quadrants [22].

2.3.2 Circular Polarization

Let's consider a case when both constituent waves have equal amplitudes, *i.e.*, *E*$_{0x}$=*E*$_{0y}$=*E*$_0$, and equal phase difference ε= -π/2 + 2mπ, where m= 0, ±1, ±2, … . The wave can be represented as

$$\vec{E} = E_0[\hat{\imath}\cos(kz - \omega t) + \hat{\jmath}\sin(kz - \omega t)]$$

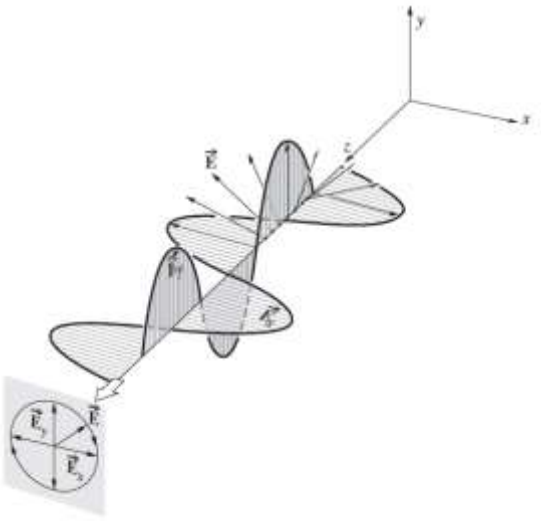

Figure 13 – Right-Circular Light. Here the electric field has a constant amplitude and rotates clockwise with the same frequency with wich it oscillates [22]

As seen in *Figure 13*, the scalar amplitude of $\vec{E}$ is a constant E_0. What varies along time is the direction of $\vec{E}$. At some arbitrary point z_0 and time t=0, $\vec{E}$ lies along the reference axis in *Figure Xa*, and numerically

$$\vec{E}_X = \hat{\imath} E_0 \cos kz_0$$

and

$$\vec{E}_y = \hat{\boldsymbol{\jmath}} E_0 \sin kz_0$$

At a time, $t=kz_0/\omega$, $\vec{E}_x = \hat{\imath} E_0$, $\vec{E}_y = 0$, and $\vec{E}$ is along the *x*-axis. The resultant vector rotates clockwise at an angular frequency of ω, as seen by an observer toward whom the wave is moving. There are two different conventions for handedness of circular polarization of light: a) from the point of view of the source (used by IEEE, and Quantum Mechanics) and b) from the point of view of the receiver (used by SPIE and older optics textbooks). Here we will consider handedness from the point of the view of the source: using the right hand, if the thumb points in the direction of propagation of light and the the fingers point in the direction of rotation of the electric field, then the light is Right (R) circularly polarized. If the left hand needs to be used for the fingers to match the direction of rotation of the electric field when then thumb points in the direction of propagation of the light, then the light has Left (L) polarization. In this case, the wave in *Figure 14* is right-circularly polarized or right circular light.

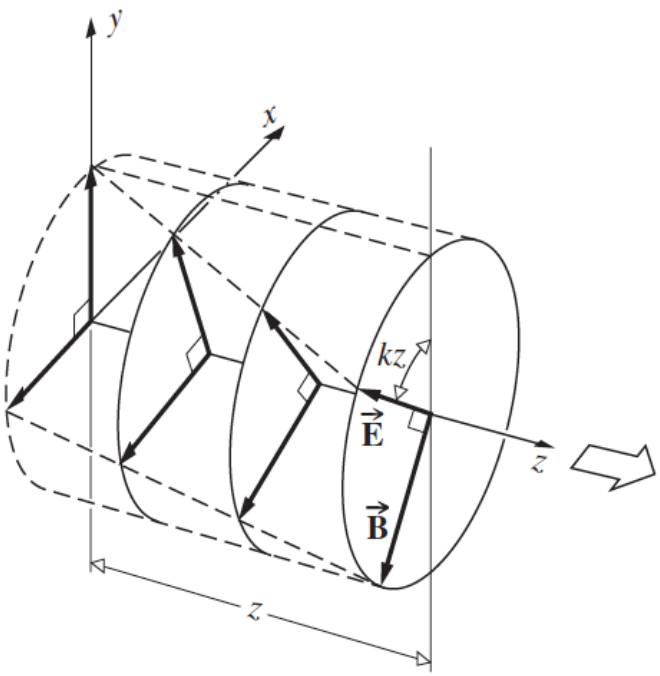

Figure 14 – Right- Circular Light. Looking down the *z*-axis toward the origin, it can be seen the electric field vector rotating clockwise as the wave advances [22]

On the other hand, if ε = π/2 + 2mπ, where m= 0, ±1, ±2, …, then

$$\vec{E} = E_0[\hat{\imath}\cos(kz - \omega t) - \hat{\jmath}\sin(kz - \omega t)]$$

The amplitude is unaffected, but **E** now rotates counter clockwise, and the wave is left-circularly polarized.

2.4 Breast Cancer

Excluding skin, in the United States is the most common cancer among women [23]. In western countries it is the most commonly diagnosed malignancy in women [24]. Early stage breast cancer is usually asymptomatic with common clinical signs as axillary mass, nipple discharge, or bleeding. It can be diagnosed via screening programs (mammography and MIR), and laboratory tests.

When diagnosing a patient, the most important factor in the overall survival (OS) rate is the stage. For example, from a 5 years range from >95% in stage I to <15% in stage IV diseases. For early stage disease, breast-conserving therapy and radiation therapy is the preferred approach. Chemotherapy further improves OS in selected stages I-IIA cases. For advanced breast cancer, mastectomy followed by chemotherapy with/without radiation therapy is the treatment of choice [24].

2.4.1 Breast Radiotherapy

Tumour site, size, grade, breast size and as well as other many factors, influence in the choice of treatment, as also the consideration of the expected cosmetic result. Recommendation for radiotherapy is made for all patients after breast conservative surgery [25] (BCU), mastectomy (depending on the size of the tumour), and in the case that the cancer has spread to other parts of the body (*e.g.* bones or brain).

The are several types of treatments. The most traditional is the conventional and standard is the whole breast radiation treatment delivering a total dose of 50G **[. Salvajoli]**, 5 days a week (2Gy per fraction) with a total extension for about 5 to 6 weeks. This treatment is supported under the radiobiologic consideration that radiation damage to normal tissue is greater with larger fraction size without additional TUMOUR control, but the extension of the treatment is an inconvenience to the patient and it has a high cost. Alternatively, hypofractionated whole breast radiation therapy (HF-WBI) delivers larger doses in typically for only 3weeks. It improves the patient quality life by lower healthcare and treatment time [24], [26]. The common dose-fractionation scheme is 42.5 Gy in 16 fractions (2.65 Gy per fraction). In some cases, TUMOUR bed boost is required after the treatment is finished commonly delivering 9 Gy in 3 sequential fractions of 3 Gy to the lumpectomy cavity [26].

2.5 Skin

2.5.1 What is Skin?

The skin, which is the largest organ of the body comprising about 16% of the body mass, and as seen in *Figure 15*, it has a very complex structure that consists of many components such as veins, capillaries and nerves [27]. Skin is divided into two primary layers, epidermis and dermis. The epidermis is the outermost layer and serves as the body's point of contact with the environment. Epidermal biological and physical characteristics plays an enormous role in resistance to environmental stressors such as infectious pathogens, chemical agents and UV [6]. Differently, the dermis underlies the epidermis and contains cutaneous structures including hair follicles, nerves and sweat glands. The dermis also contains immune cells and fibroblasts, which actively participate in many physiologic responses in the skin.

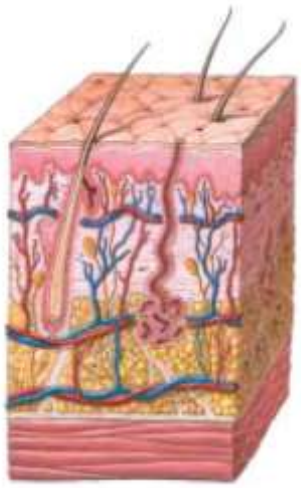

Figure 15 – Skin structure [27]

The functions of skin varies in degrees according to age, race and gender. For example, older skins might los its flexibility and toughness. The light-protection ability of skin among races varies because of differences in the volume of melanin which absorbs ultraviolet light.

2.5.2 Skin Toxicity

Radiotherapy is an elementary step in a breast cancer treatment, and during the course of breast cancer radiotherapy, between 74% and 100% of patients will experience radiodermatitis (as known as, skin toxicity) [25] , [28]. It can be physically manifested from a faint erythema (redness, rash-like appearance), to dry and moist desquamation, or even necrosis. After a treatment is concluded, patients may experience skin texture, discomfort, pain, and itching. It also affects the patients life quality, by disturbing body image, by causing sleep problems and emotional distress. Therefore, control of skin toxicity in three-dimensional Radiation Therapy, IMRT and Tomotherapy is crucial because it could lead to temporary cessation of the treatment [29].

Radiation dermatitis develops in a predictable timing and in a dose dependent way. The most common skin reactions are for example: follicular reaction with pruritus, skin erythema, dry desquamation and moist desquamation in the inflammatory fold as seen in *Figure 16*. Clinical symptoms can be seen *Table 2*.

Figure 16 – Common Skin reactions in patients undergoing breast radiation therapy. (A) Follicular reaction with prutitus. (B) Skin erythema and edema. (C) Dry desquamation. (D)

Table 2 – Clinical Symptoms of Acute Radiation dermatitis

Skin Reaction	**Onset**	**Dose Threshold (Gy)**
Erythema	7-10 days	6-10
Dry Desquamation	3-4 weeks	20-25
Moist Desquamation	4+ weeks	30-40
Ulceration	5+ weeks	>40

The first clinically skin change after breast irradiation is erythema, which it can be appreciated some hours after irradiation. The most typical skin reaction occurs 10 to 14 days after initiation of irradiation and often will worsen throughout the course of treatment. Desquamation, either dry or moist, appears with higher radiation doses in the final part of the treatment on course.

Methodology

3.1 Patient Selection

This research had to be approved by the Ethical Committee of the Faculty of Philosophy, Sciences and Letters of Ribeirão Preto, of the University of São Paulo, and the Ethical Committee of the Ribeirão Preto Medical School (HCFMRP-USP) (CAAE nº 73541017.20000.5407). It included 23
breast cancer patient over 18 years old that had undergone any of the three following photon radiotherapy: conventional treatment and hypo-fractionated treatment . The patients were treated five times a week to a total dose depending on the treatment.

Based on the Fitzpatrick scale [6], patients of all pigmentary phototype were chosen to participate in the study. Also patients with none, partial or total mastectomy were included, as well as patients with all type of breast size.

3.2 Camera

The camera used for image acquisition was a Casio EX-10 (*Figure 17*). Its specifications are in Appendix C, *Table 3.*

Figure 17– Casio EX-10 Camera

3.3 Polarizer

A circular polarizer (right handed) sheet was used in the image acquisition. It was located in front of the flash and the camera lens. The specifications of the polarizer sheet are in *Appendix C, Table 4.*

In the *Figure 18* appears the configuration of the polarizers used for the image acquisition of the images. Light does not go very far to the right side of the second polarizer. In practice, some light leaks (0.5% leak transmission with polarizers used) because of the quality of the polarizers. The symbol on the left represents a light source, the following two pairs of boxed lines represent two right polarizers, and the line in the middle represents a R-polarized light wave.

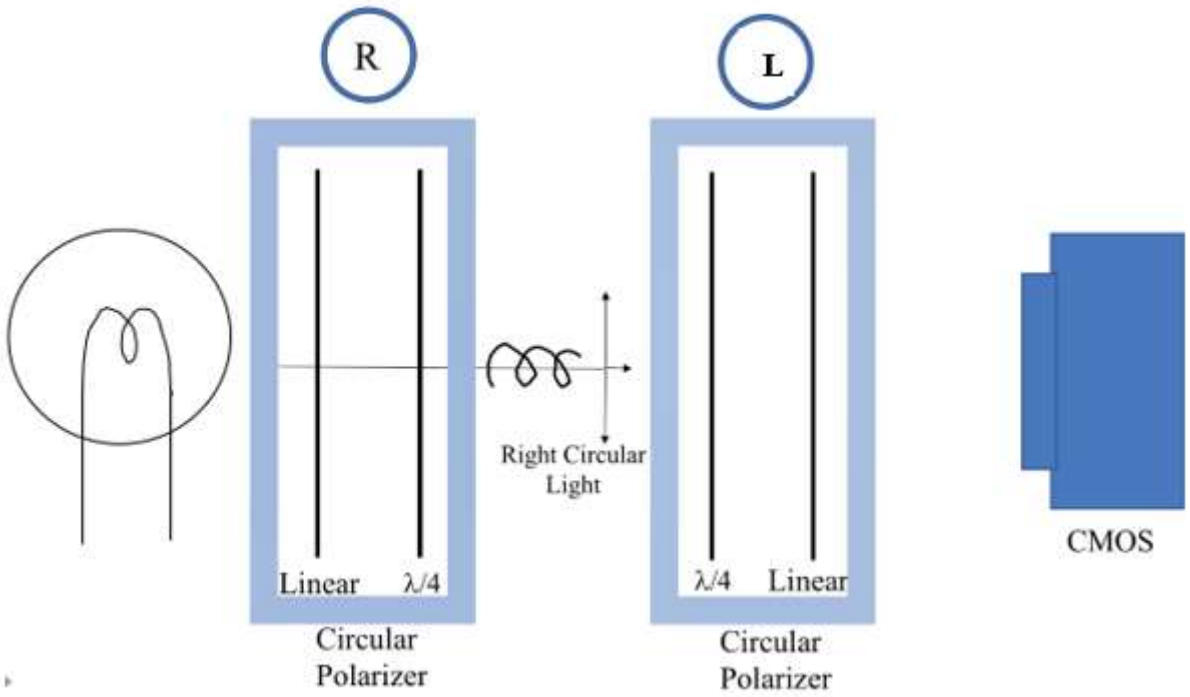

Figure 18 – Configuration of the polarizers used for image acquisition

The circular polarizing sheet is comprised by a linear polarizer which and a layer of λ/4 (quarter-wave plate). This quarter-wave layer is calculated to an intermediate wavelength, around the green. Thus, for longer or shorter wavelengths we have an elliptical (not circular) polarization.

In the *Figure 19* appears the effect of a specular reflection and diffuse reflection. Specular reflection turns R polarization into L polarization. However, with penetration and scattering inside the skin the light loses polarization, diffuse light exits with both R and L components. Therefore the specular reflection turns into L and does not cross the polarizer in the camera, while light that images the subepithelial tissue contains roughly equal parts of R and L -

polarized light, reaching the camera. This results in a simplification of the setup and the imaging of the sub-epithelial tissue can be done with a single layer of R or L polarizer that covers both the illuminator and camera. The position of the quarter-wave plate must be on the opposite side both from the illuminator and from the camera lens.

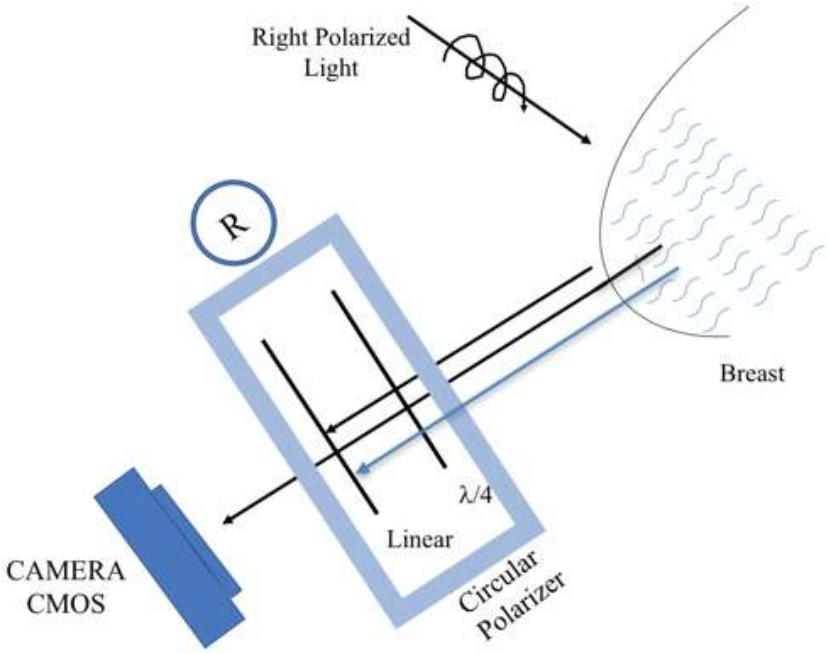

Figure 19 – Effect of specular reflection

The circular polarizing sheet is comprised of a linear polarizer which it was included a delay layer of λ/ 4 wavelength. This quarter-wave layer is calculated to an intermediate wavelength, around the green. Thus, for longer or shorter wavelengths we have an elliptical (not circular) polarization.

3.4 Image Acquisition

It is expected that during the treatment there is going to be a cumulative damage to the skin and that it will become redder. Considering the acquisition of images during the treatment, it is contemplated that the intensities of the image are going to change according to accumulated dose.

Follow-up of the patient's skin colour evolution was evaluated with photographs at the beginning of treatments (before being treated), throughout the treatment, 1 to 5 times a week, in random days, and one week, and 4 weeks after finishing. Digital and polarized images were used in this study and their intensities in different colour spaces were evaluated and correlated to the qualitative method using the RTOG schema.

Images were obtained for each patient in random days. One of our hypothesis is that as the delivered dose is linear, the skin damage will appear linearly as well. So for example, for a hypo-fractionated breast cancer patient, images were obtained in the first and last day of treatment, in their medical return; and in different days along the treatments, as seen in *Figure 20.*

Figure 20 - Example of Image Acquisition for a hypo-fractionated patient

The images were taken in a room without windows inside the radiotherapy service. It was right next to the treatment room so the patients should not have to walk too much. Inside, they were seated in a wooden bench where they supported their backs on the wall. They bench and the camera tripod was always located in the same place every day and for all the pictures (*Figure 21).* Before each image, it was shown to the patient the image of the first day so they could repeat the same position of the arms. Even though this was done, many patients cause of their age, previous breast surgery and/or arm pain; were not able to maintain the same positions for too many seconds. Also it is important to consider the differences in the images from one day to another cause of breath movement.

Figure 21 – Tripod setup and localization for each day of the image acquisition. Marks were located in the floor for each type of image, and also in the wall.

Digital photographs were taken from 3 different positions to reach all regions of the treatment field, frontal, lateral and below the breast (*Table 5*). For each position, pictures were taken with or without room light, when the room light was off, the camera flash was used. For both conditions, a photo was taken with non-polarized light and a photo with light circularly polarized orthogonally to a polarizer positioned on the camera lens.

Table 3 – Image Acquisition Set Up

FRONTAL IMAGES ACQUIRED			
			
LATERAL IMAGES ACQUIRED			
			
GROOVE IMAGES ACQUIRED			
			

The polarized images were used in this study to eliminate the oiliness influence in the comparison of intensity values between different patients and also in a try to detect some subsurface skin information that can be used to predict any radiodermatitis, allowing a better patient care during the treatment. In *Figure 22*, it can be seen the setup of the polarizers and the camera. A circular polarizer was placed in front of the flash camera, and another in front of the camera lens. When combining both polarizers, it was similar to a perpendicular polarization.

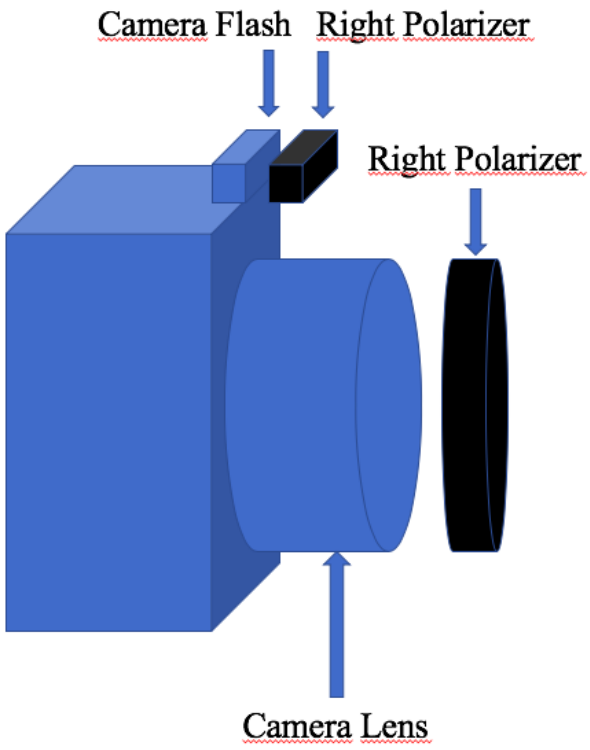

Figure 22 - Camera Set up for image acquisition. A right circular polarizer was located in front of the camera lens and flash.

3.3 Image Processing

All the images were processed using MatLab software, by a study of the intensity values of specific regions of interest (ROIs) in RGB colour along time of the treatment.

Taking advantage of anatomical regions, skin marks and tattoos in the border of the treatment field on the patients, an image registration based on geometric transformation was done [30] .

For each patient the reference points were chosen individually. The first of a set of images for a whole treatment was used as reference, so their points were named as *rixed points.* For all the other images, the points were named as *moving points*. MatLab offers a function for doing the geometric transformation called “fitgeotrans”. So the code used was:

```
tform= fitgeotrans(movingpoints,fixedpoints,'affine');
```

Image to be registered

Fixed Image

Type of geometric transformation

After the geometric transformation is defined, it has to be applied to the image as follow:

```
Jreg=imwarp(IM_2,tform,'OutputView',imref2d(size(IM_1)));
```

Image after registrarion

Image to be registered

Fixed Image

Usually the tattoos of the border of the treatment field were used on the registration, *figure X-a* shows them for a lateral image of a hypofractionated patient

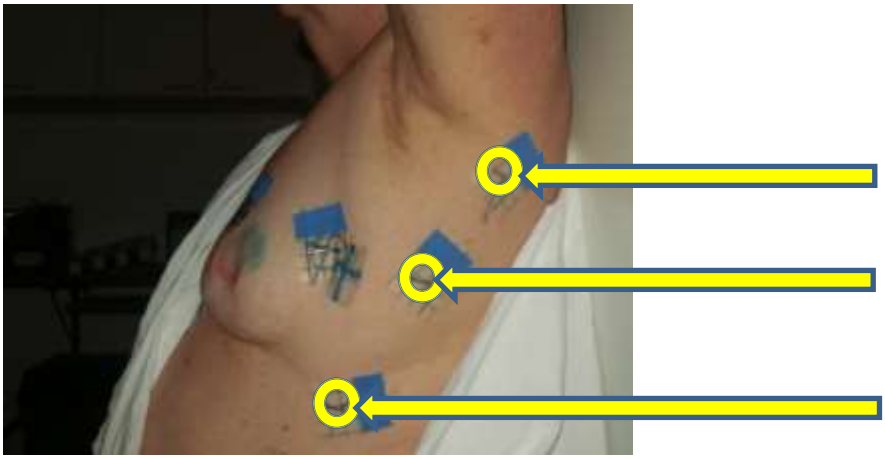

Figure 23 – Reference points for geometrical transformation.

All the images acquired for each patient were registered to find the ROI where at least grade 1 RTOG radiodermatitis was identified. The RTOGs assessment was done by any of the radiation therapists residents from the radiotherapy service.

This ROI was manually selected in the first image of the treatment in Matlab. Then, automatically the same ROI at the same position was selected in the registered images. For each ROI, it was calculated the mean of the pixel intensity in each channel for each space

colour, i.e., RGB, HSV, and La*b*. At the same time, this ROI was normalized by the mean intensity of a white stripe located outside the treatment area. This stripe was used in all the images for all the patients along their treatment (*Figure 24).*

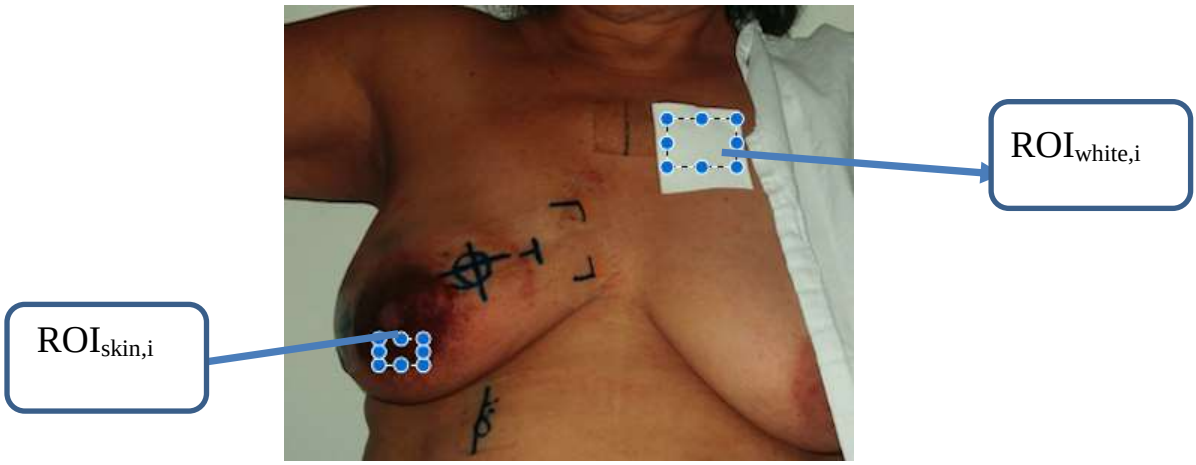

Figure 24 – ROI selected in the treated area, and the ROI of the white stripe located outside the treatment area.

Normalizing by the white stripes helps in deleting differences in the flash camera intensity, because it is known that the light variates depending on the position. Also, as the camera was set in automatic mode, the illumination one day from another also variated. This idea is based on the work of Levine M.D, and Bhattacharyya J. [30]

3.3 Statistical Methods

T-test was used to study the behaviour of the ratio means of the different types of skin. A P-value of less than 0.05 was considered statistically significant. Outlier values were excluded from the analyses.

Results and Discussion

This section of the text will be divided in three parts. Firstly, a qualitative discussion about issues related to the methodology used in this study is going to be presented; secondly, the results and its discussions will be presented and finally, the limitations of this study are going to be discussed.

Initially, when this study was designed, it was proposed that polarized and non-polarized images were going to be taken of the patients and these images were acquired. However, a visual examination of them showed the advantages of the images obtained in a dark room with the circular polarizer, where the polarization helps to eliminate the superficial glare, thus, the skin can be studied without the noise generated by the light that reflexes in the skin. As well, physicians found an important difference between the images. For example, for the first patient in the lateral image in the 16^{th} fraction, it can be seen in *Figure 25*, an image with room light and non-polarized light. The axilla appears slightly red. The region next to the scar still doesn't have a grade 1, but it is hyperchromic. Moving forward on the images, when using room light and polarized light, the region looks more redder. For the image without room light and non-polarized light, the treated area look more precisely. At last, the image without room light and polarized light shows better the extension of the lesion, and in the transparent stripes helps positioning the patient in the treatment couch, it can be seen there is no reflexion compared with the anterior image.

(a) Lateral Image with room light and non-polarized light.

(b) Lateral Image with room light and polarized light.

(c) Lateral Image with without room light and non-polarized light.

(d) Lateral Image with without room light and polarized light.

Figure 25 – For the 1st patient: (a) Lateral image with room light and non-polarized light, (b) Lateral image with room light and polarized light, (c) Lateral image without room light and non-polarized light, (d) Lateral image without room light and polarized light.

This study also used small ROIs, just selecting the region where in fact a RTOG erythema appeared on the breast, the decision for using them was based on the failure of other proposed methodologies when applied to our data. As an example, we tried to evaluate our data following the study of Wensgtrom *et. al.*, that proposed the segmentation of the breast area in a frontal image in 5 regions, as seen in *Figure 26*, for analysing the pixel intensity variation during the treatment [15].

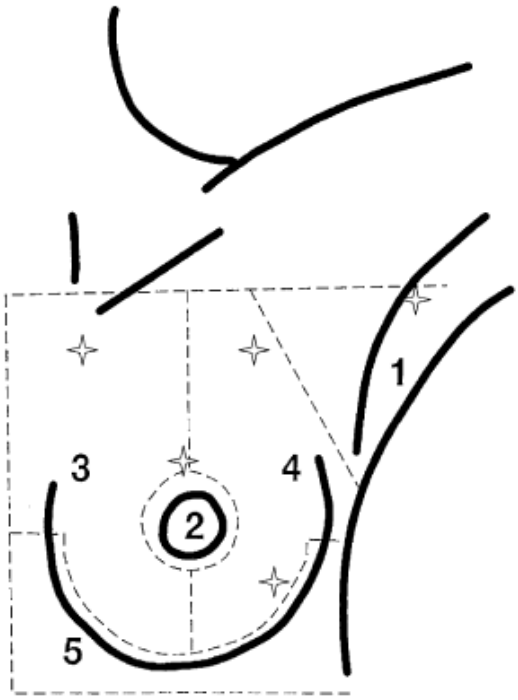

Figure 26– Breast Skin treated area divided in 5 anatomical sections: (1) axilla, (2) areola, (3) medial breast, (4) lateral breast, (5) inframammary fold [15].

This methodology was tried in our results, but some difficulties were found:

- This segmentation is not possible in patients with partial mastectomy, because the nipple is removed, and there is not inframammary fold.
- This segmentation is not possible in patients with total mastectomy, because the nipple is removed, there is no inframammary fold, and depending independently of each patient, there is a scar in a different position and it has a different size.
- This segmentation is not possible for patients with big breast, because the inframammary fold covered by the breast, and in many occasions, the breast has the nipple on the tip of the breast (*Figure 27)*, and this cases, the axilla is hard to see in the frontal image.

Figure 27 - Frontal Image of a patient with big breast. It can be seen that the orientation form of the breast does not agree with the one proposed to be analysed by

Because of this, is that images were obtained in three lateral positions, so it could be seen the hole treatment area. On the other hand, trying to solve the problem of big breast patients that covered the inframammary fold, images were obtained asking the patient to push their breast every day in the same position, but when they hold their breast, every day they grab it in a different position, making it almost impossible to reproduce the image of the first day, as seen in *Figure 28*. Also, when the patient grab their breast, they pressed their skin, changing the skin colouration, making the inframammary fold images unusable.

(a) Groove Image in the 11th fraction of the patient 7

(b) Groove Image in the 13th fraction of the patient 7

(c) Groove Image in the 14th fraction of the patient 7

(d) Groove Image in the 16th fraction of the patient 7

Figure 28 – For the 7th patient, groove images of the: (a) 11th fraction, (b) 13th fraction, (c) 14th fraction, (d) 16th fraction.

At last, for various patients with no partial or total mastectomy, it was tried to applied Wengström methodology. As seen in *Figure 29*, we studied the histogram of the medial breast region of the patient 1.

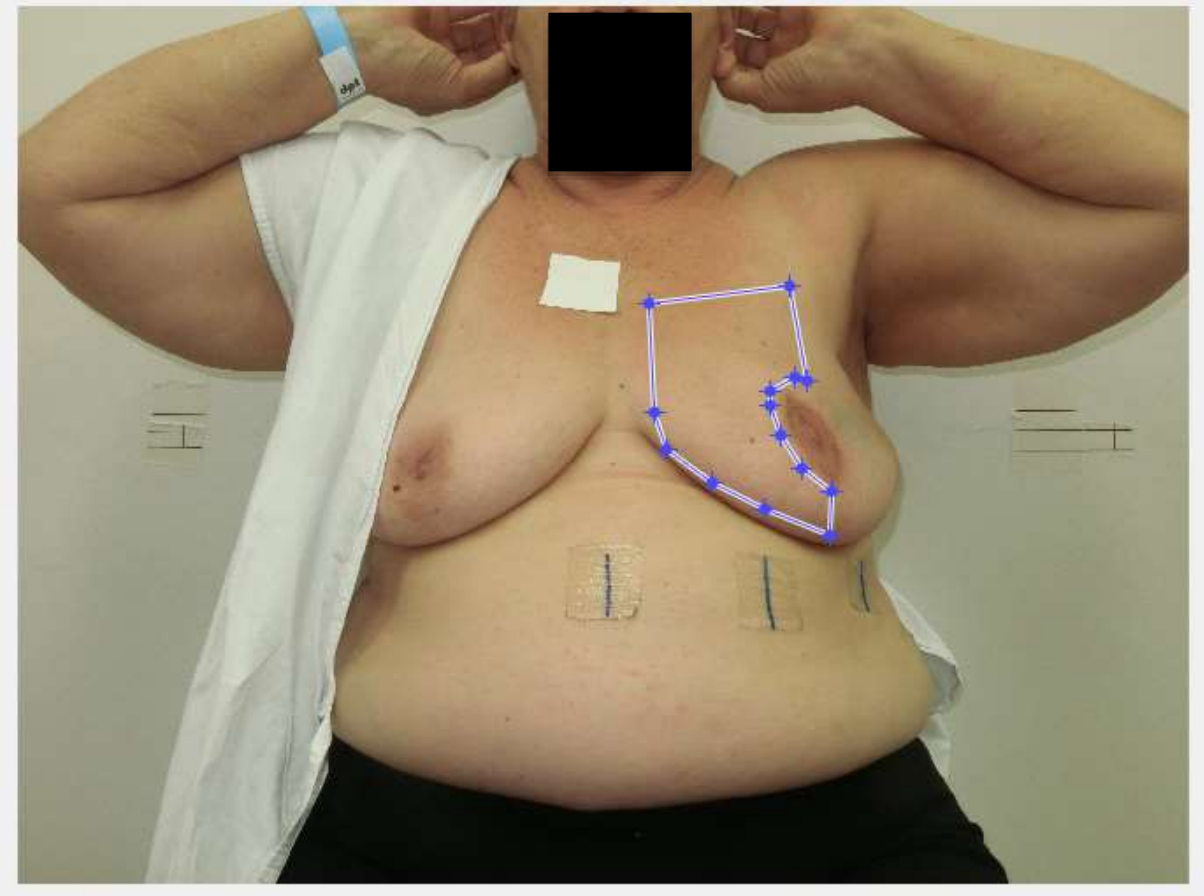

Figure 29 – Medial breast ROI selection for image analysis

The histograms obtained can be seen in *Figure 30*. The green channel is studied in all the treatment fractions, where the *x* axis is the pixel intensity normalized by the white stripe (Normalized Histogram), and the *y* axis is the pixel count for each value. In the histogram of the 3th fraction, the shape has 3 peaks. In the 8th fraction, the middle peaks appears more pronounced, and the first peak from left to right disappears. For the other fractions, the peaks appears more pronounced as well as that their a displacement of them. The displacement shows us that in fact the pixels gets darker, and about the histogram shape modification along the treatment, that there are different regions inside a single anatomical section, that gets redder independently one from another. So its non-viable to analyse a full region as Wengstöm did. Even when studying a small anatomical region, different peaks appear in the histogram

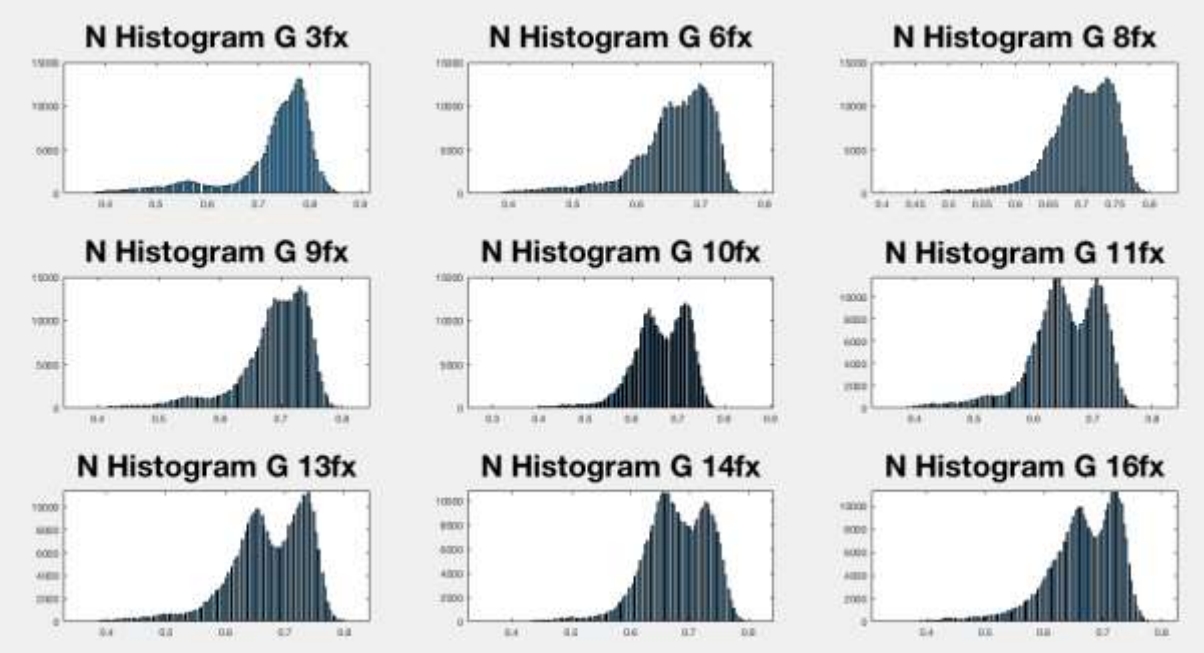

Figure 30 – Histogram of the medial breast of patient 1. The green channel is analysed throughout the treatment. The peaks of each day changes in form and they translates to the left along the treatment.

Now, after understanding which images and ROIs will be studied, we will start presenting the results for one patient in one particular position as an example of the procedure applied for all patients. The patient number 10 of the study underwent a hypofractionated treatment. She has white skin and before starting radiation therapy, she had a total mastectomy surgery. Her pictures were obtained in the fractions 3, 4, 5, 6, 7, 9, 12, 13, 15 and 16; and one week after finishing her treatment. No boost was applied.

The images obtained along the treatment in the lateral position and using the circular polarizer are shown on *Figure 31*.

(a)

(b)

(c)

(d)

(e)

(f)

(g)

(h)

(i)

(j)

(k)

Figure 31 – Lateral Image of the 10th Patient in the fraction number: (a) 3, (b) 4, (c) 5, (d) 6, (e) 7, (f) 9, (g) 12, (h) 13, (i) 15, (j) 16 and (k) one week after finishing the treatment.

The ROI analysed along the treatment is presented on *Figure 32*. For all the pictures achieved along the treatment, the mean pixel intensity of the ROI was normalized by the mean value of the pixel intensities of the first day, and this procedure was done in each RGB channel (*Figure 33).* It is possible to see that the normalized intensity value decreases as the treatment evolves for all the three channels, result that is expected, since the skin gets darker or redder as it receives the radiation, depending on the skin type.

In the first 6 images the ROI has a grade 0. Between the 14th (12 fraction) and 21th (13 fraction) day, the skin has a grade 1. The time between this two fractions is considerable due to the hospital scheduling which was affected in the study by public holidays, Linear Accelerator Q&A, and problems in the machine.

The patient 10 finishes the hypofractionated treatment after 3 weeks, in the 25th day. One week after in the medical return, she continuous with a grade 1 in the ROI, but the ratio value is lesser than when the treatment finished. This agree with other research studies that state that in hypofractionated treatments, the skin will have a late skin reaction [29].

Figure 32 – ROI analysed for the lateral image of patient 10.

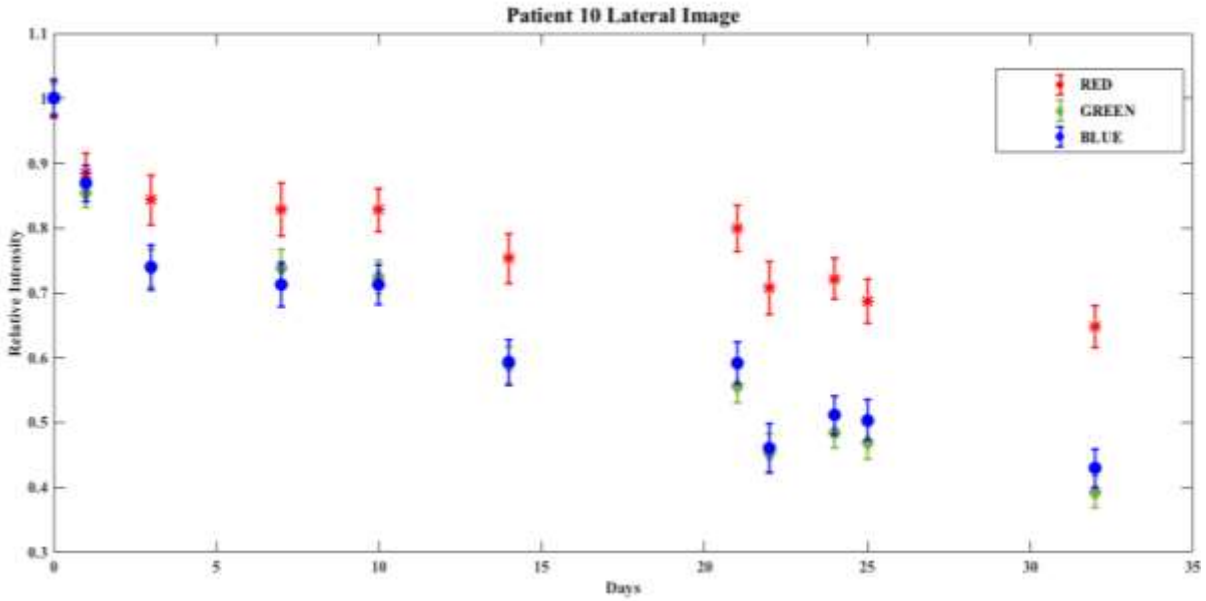

Figure 33 – Relative Intensities for the patient 10. Until the 14th day, the patient has a RTOG grade 0. The following days, including the medical return on the 32th, the patient has a RTOG grade 1.

For the same patient, grouping the ratios for each grade, we finally obtain as seen in *Figure 34*, a plot that shows how each channel of the RGB behaves for each RTOG grade. For grade 0, as we are studying a normalized ratio, all values keeps closer to 1. For grade 1, the red channel is less sensitive that the blue and green channel.

Grouping the ratios for each grade, by calculating the mean value of normalized intensities for each radiodermatitis grade, we finally obtained the range of normalized intensity values for this patient. The grade 0 presented mean intensities values of 0.86±0.04 , 0.77±0.03 and 0.77±0.04 for the R, G and B channels respectively, while for the grade 1 radiodermatitis the values are 0.71±0.03 , 0.47±0.03 and 0.50±0.03 for the R, G and B channels respectively. For the same ratios presented before, the normalized intensity values decreases as the radiodermatitis grades increases

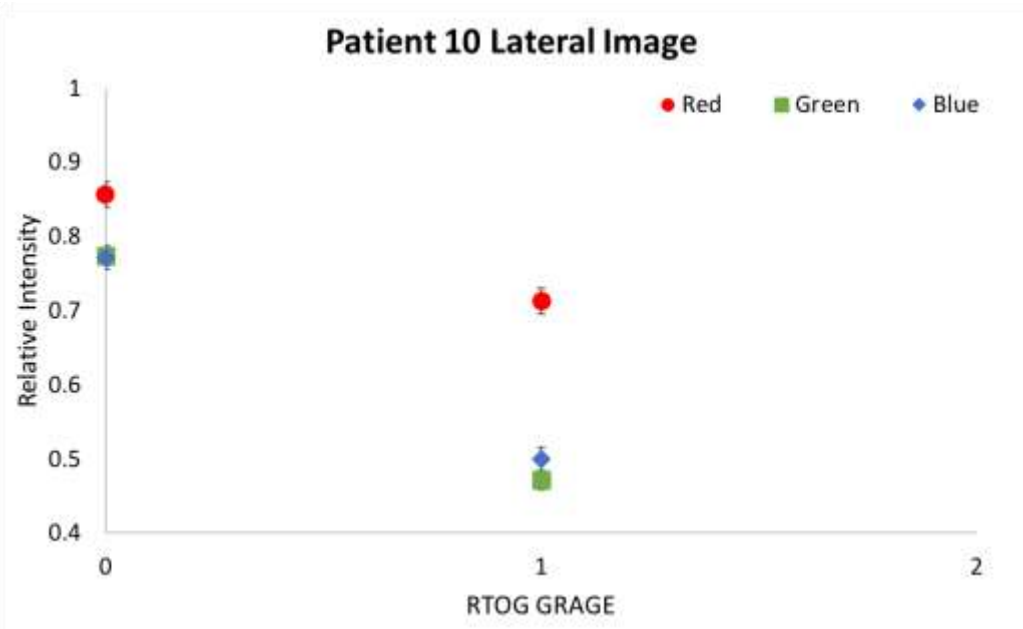

Figure 34 – Relative Intensity versus RTOG grade for the patient 10

This procedure was repeated for all the patients, figure 35-69 presents one image of patient with the analysed ROI (a) and the final graph of the relative intensities versus the RTOG grade (b).

Patient 1

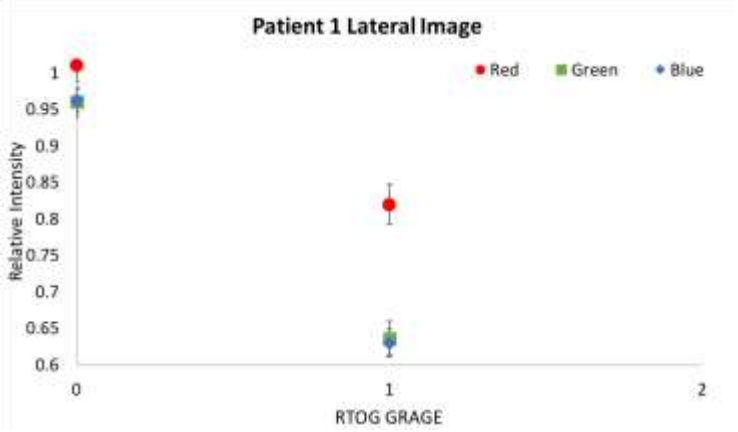

(a) (b)

Figure 35 – (a) An example of the pictures achieved for patient 1, and the analysed ROI positioning. (b) Mean values of the relative intensities versus the RTOG grade.

Patient 1 has white skin. It is expected that the skin will have a severe reaction to radiation. At grade 1, the lesser sensitive channel is the red channel. Both green and blue channel has a ratio close to 0.65

Patient 2

(a) (b)

Figure 36 – (a) An example of the pictures achieved for patient 2, and the analysed ROI positioning. (b) Mean values of the relative intensities versus the RTOG grade.

Patient 2 was included in the study in the end of its conventional treatment. Even though the patient has a grade 1 below the mastectomy scar, the ratio for the 3 channels is above 1, showing how each patients reacts differently.

Patient 3

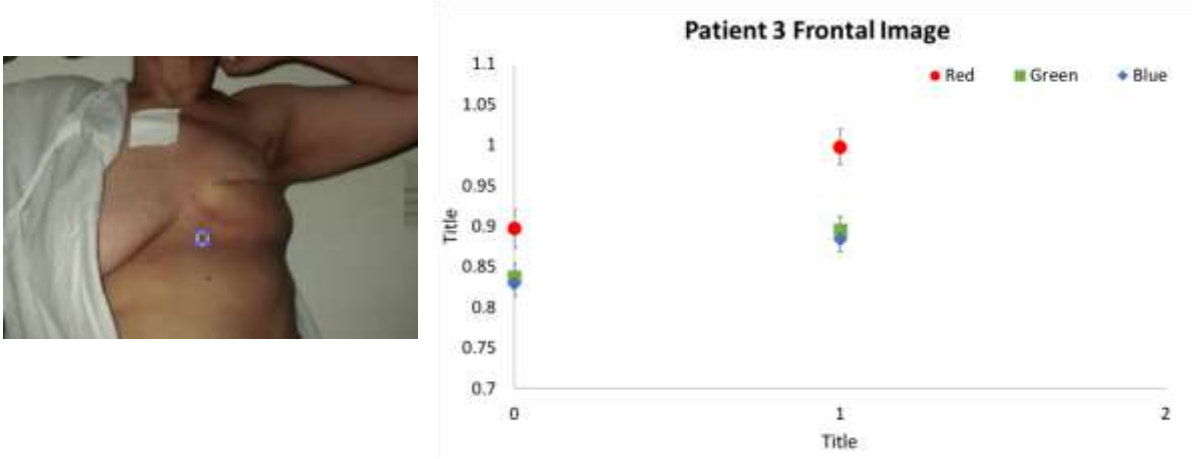

(a) (b)

Figure 37 – (a) An example of the pictures achieved for patient 3, and the analysed ROI positioning. (b) Mean values of the relative intensities versus the RTOG grade.

Patient 3 has brown, and in comparison with Patient 1, for a grade 1 in the frontal image in the inframammary fold, the ratio is no lower than 0.9. The red channel is above 1.

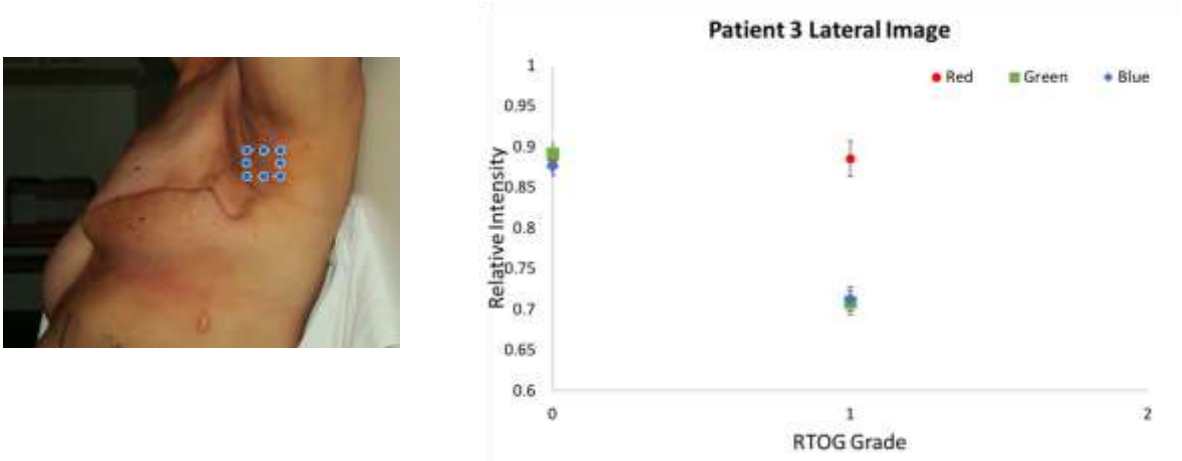

(a) (b)

Figure 38 – (a) An example of the pictures achieved for patient 3, and the analysed ROI positioning. (b) Mean values of the relative intensities versus the RTOG grade.

For the same patient, in the lateral image, the ROI in the armpit has a grade 1. The channel R keeps almost constant for both grades, but the channel G and B have a value of about 0.7

Patient 4

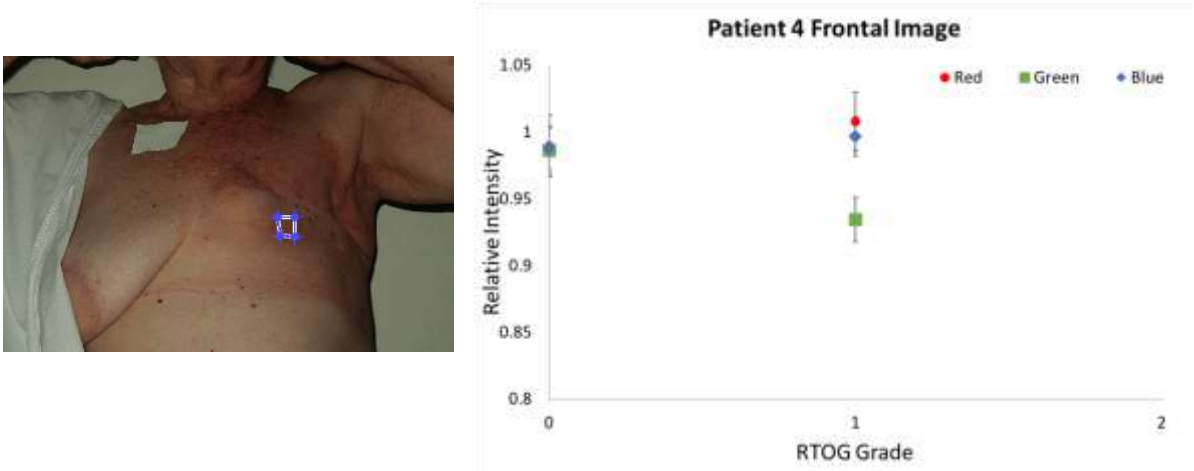

(a) (b)

Figure 39– (a) An example of the pictures achieved for patient 4, and the analysed ROI positioning. (b) Mean values of the relative intensities versus the RTOG grade.

Patient 4 has white skin, and as for Patient 1, a higher radiodermatitis was expected. In the end of the treatment the patient had a mild grade 1, where only the channel G had a value lesser than 1.

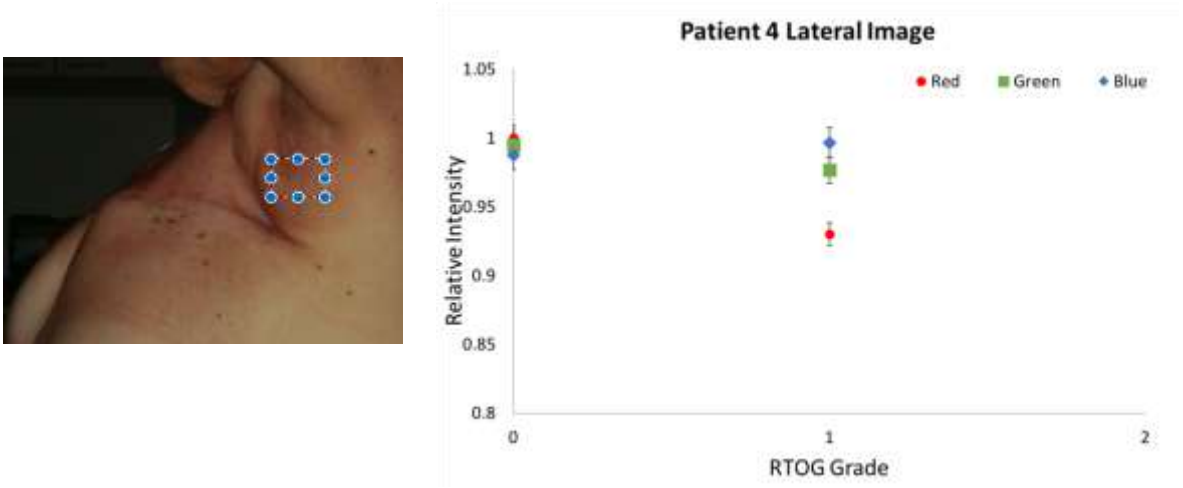

(a) (b)

Figure 40 - (a) An example of the pictures achieved for patient 4, and the analysed ROI positioning. (b) Mean values of the relative intensities versus the RTOG grade.

For the same patient in the arm pit, the RGB values do not decline as expected.

Patient 5

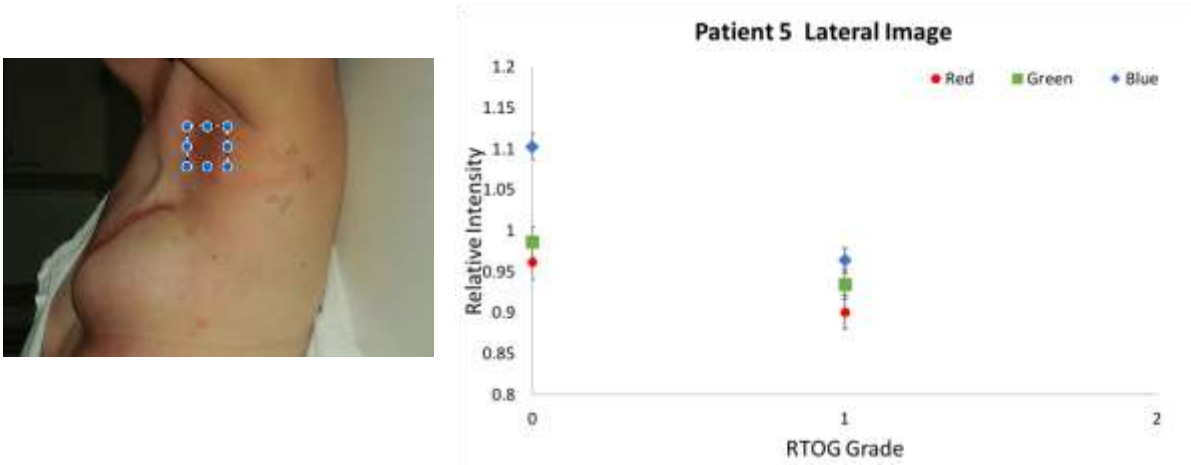

(a) (b)

Figure 41 – (a) An example of the pictures achieved for patient 5, and the analysed ROI positioning. (b) Mean values of the relative intensities versus the RTOG grade.

Patient 5 as well has white skin, having a mellow grade 1 in the arm pit. Again the RGB channels don't decrease as expected.

Patient 6

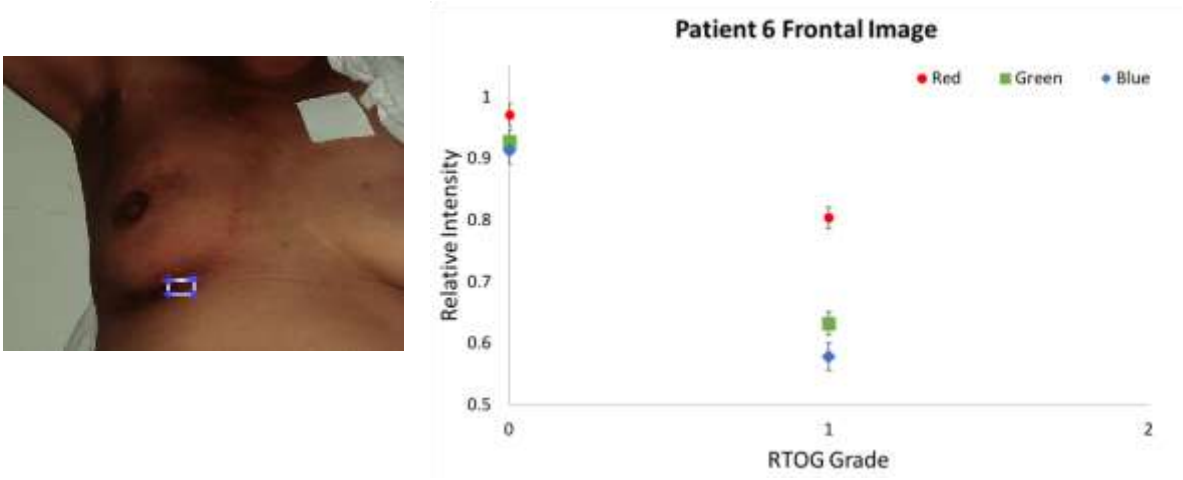

(a) (b)

Figure 42 – (a) An example of the pictures achieved for patient 6, and the analysed ROI positioning. (b) Mean values of the relative intensities versus the RTOG grade.

For a brown skin patient with a grade 1 in the inframammary fold, the diminution in the ratio is more accentuated than in patients with white skin. The green and blue channel have a value close to 0.6

Patient 7

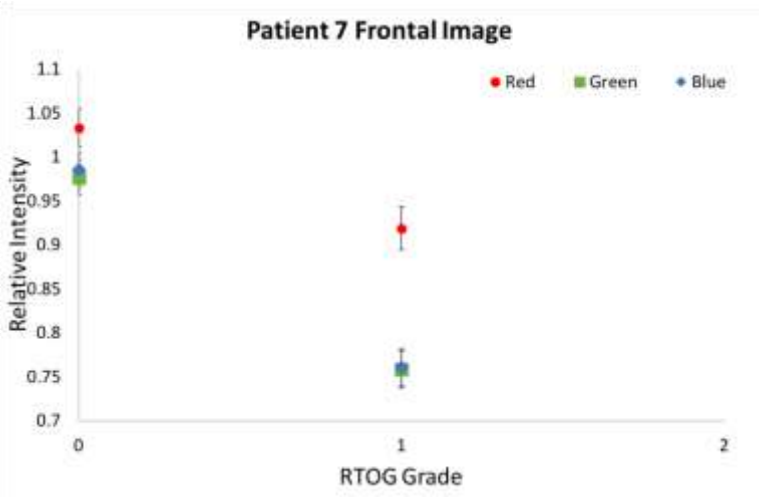

(a) (b)

Figure 43 – (a) An example of the pictures achieved for patient 7, and the analysed ROI positioning. (b) Mean values of the relative intensities versus the RTOG grade.

A brown patient with grade 1 in a frontal image presents a diminution in the green and blue channel with a value nearly to 0.75.

Patient 8

(a) (b)

Figure 44 – (a) An example of the pictures achieved for patient 8, and the analysed ROI positioning. (b) Mean values of the relative intensities versus the RTOG grade.

(a) (b)

Figure 45 – (a) An example of the pictures achieved for patient 8, and the analysed ROI positioning. (b) Mean values of the relative intensities versus the RTOG grade.

Patient 8 has white skin and started and hypofractionated treatment after a total mastectomy surgery. It was expected for the higher dose per fraction, and the skin colouration, that the radiodermatitis grade in the end of the treatment and in the medical returns, that the patiend would have a grade 2 or even more. Finally, in the end of the treatment the patient had a very slight change of colour in the chest, were the physicians evaluate the skin as a grade 1, and also a grade 1 in the armpit where the ratio was more sensitive .

Patient 9

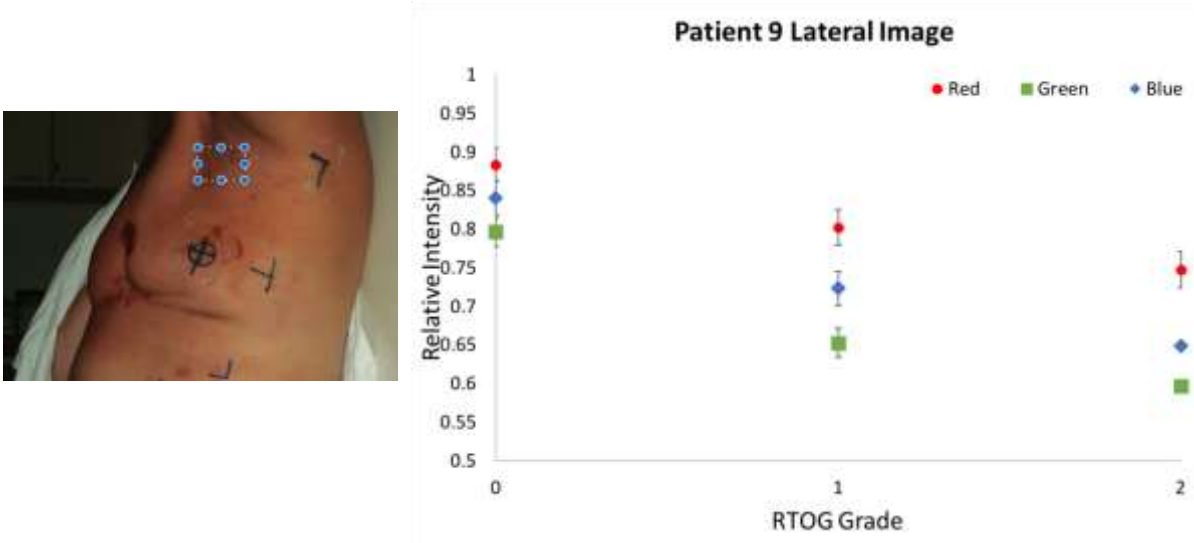

(a) (b)

Figure 46 – (a) An example of the pictures achieved for patient 9, and the analysed ROI positioning. (b) Mean values of the relative intensities versus the RTOG grade.

Patient 9 in the end of the treatment had a grade 1 in the armpit. In the first medical return the ROI still had a grade 1, and in the grade 2, the ROI had a grade 2 (*Figure 47)*. Even thought, the ratio for the grade 2 presents a decrease, were a minimum increase was expected. This is may be due by the fact that the ROI in grade 2 includes regions with grade 1.

Figure 47 – Images of one week and 4 weeks after finishing the treatment. On the left, it can be seen a grade 2 lesion with a big desquamation area in the ROI.

(a) (b)

Figure 48– (a) An example of the pictures achieved for patient 9, and the analysed ROI positioning. (b) Mean values of the relative intensities versus the RTOG grade.

For this frontal image, the region next to the mastectomy scar is analysed. A mild grade 1 appears, with a normal ratio no lesser than 0.85 for the green and blue channel.

Patient 11

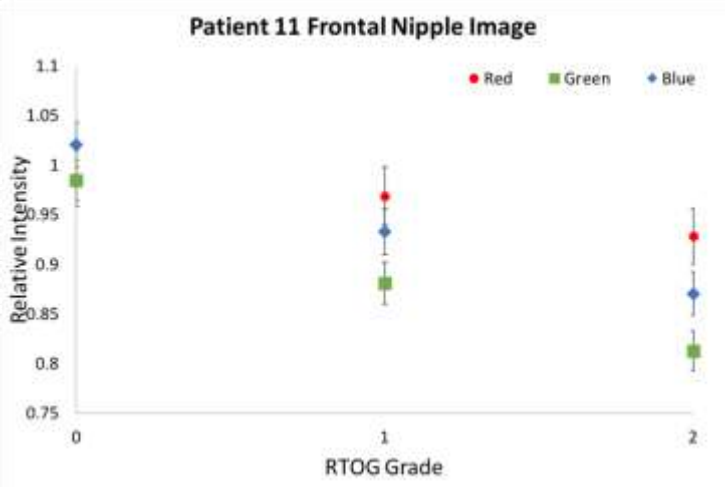

(a) (b)

Figure 49 – (a) An example of the pictures achieved for patient 11, and the analysed ROI positioning. (b) Mean values of the relative intensities versus the RTOG grade.

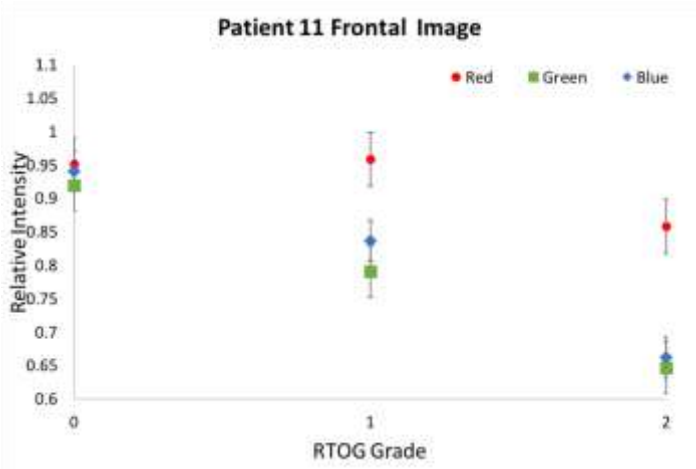

(a) (b)

Figure 50 – (a) An example of the pictures achieved for patient 11, and the analysed ROI positioning. (b) Mean values of the relative intensities versus the RTOG grade.

Patient 11 has white skin. In *Figure 49*, the nipple has a grade 2 as it desquamates in the end of the treatment. For the grade 2 value the is not an increase because the ROI included the a partial part of the nipple and the skin breast.

Beside the nipple, the patient has as well a grade 2, showing that the skin in comparison to the nipple, is more sensitive.

Patient 12

(a) (b)

Figure 51 – (a) An example of the pictures achieved for patient 12, and the analysed ROI positioning. (b) Mean values of the relative intensities versus the RTOG grade.

Patient 12 presents a grade 1 in the nipple. The ratio represents well this lesion, with values that goes form 0.8 for grade 0, up to grade 0.5 approximately.

(a) (b)

Figure 52 – (a) An example of the pictures achieved for patient 12, and the analysed ROI positioning. (b) Mean values of the relative intensities versus the RTOG grade.

Even though patient 12 presents a grade 1 in the axilla, the variation between both grade is low. Both 3 channel decreases in a same ratio.

Patient 13

(a) (b)

Figure 53 – (a) An example of the pictures achieved for patient 13, and the analysed ROI positioning. (b) Mean values of the relative intensities versus the RTOG grade.

Patient 13 has white skin. It has a grade 1 in the axilla. The red channel between both grades does not change so much, but the green and blue channel varies in approximately 0.3.

Patient 14

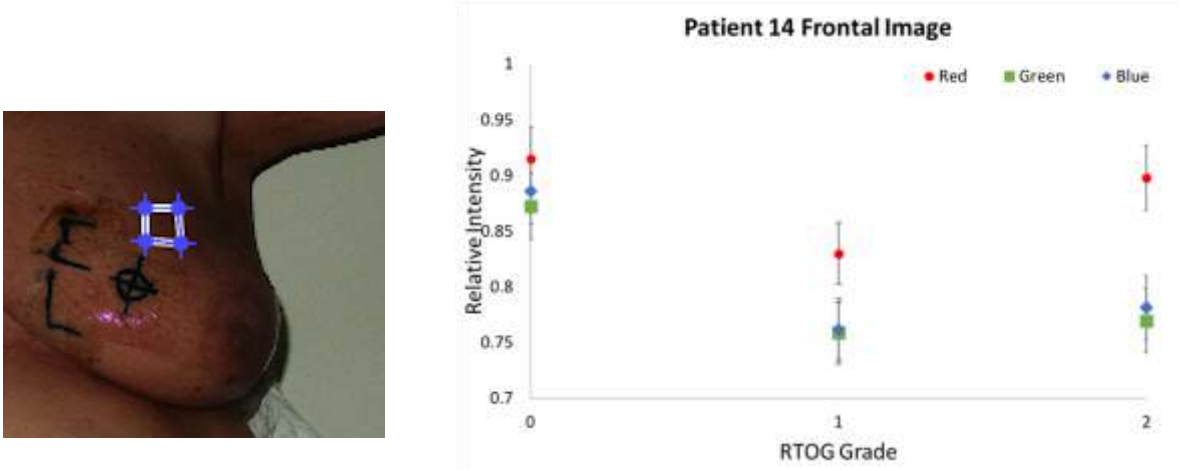

(a) (b)

Figure 54 - (a) An example of the pictures achieved for patient 14, and the analysed ROI positioning. (b) Mean values of the relative intensities versus the RTOG grade.

Patient 14 of white skin, has a grade 2 in the breast in a region close to the nipple. For grade 1, the three channels of the RGB channel diminishes, but for grade 2, there is a considerable increase in the red channel. The green and blue channel increases a little bit, confirming the idea that when there is a grade 2, in most of the cases there is a rise in the ratio.

Patient 15

(a) (b)

Figure 55 – (a) An example of the pictures achieved for patient 15, and the analysed ROI positioning. (b) Mean values of the relative intensities versus the RTOG grade.

For the frontal lateral, even though there is a grade 2 in the ROI, the ratio diminishes. This may be cause of a small grade in the region studied, not affecting in this way the pixel intensity.

(a) (b)

Figure 56 – (a) An example of the pictures achieved for patient 15, and the analysed ROI positioning. (b) Mean values of the relative intensities versus the RTOG grade.

For the frontal image, for grade 0 and 1, the ratio stays almost constant. Only for grade 2 the R channel decreases, but not as much as the green and blue channel.

Patient 16

(a) (b)

Figure 57– (a) An example of the pictures achieved for patient 16, and the analysed ROI positioning. (b) Mean values of the relative intensities versus the RTOG grade.

Patient 16 has an interesting behaviour for both lateral and frontal image. For grade 1, the ratio of the 3 channels decreases close to 0.35. For grade 2, almost the whole ROI has grade 2, which make the ratio increase up to 0.50 approximately. In this case, the channel which increases the most is the blue, then the red and at last, the green channel.

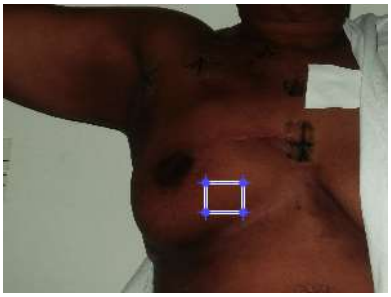

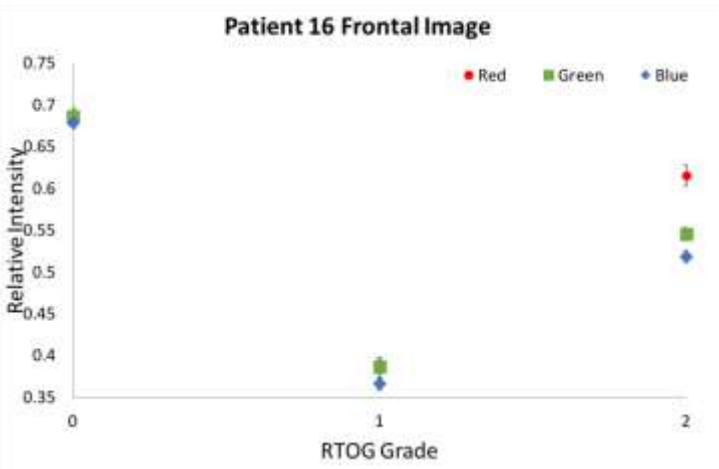

(a) (b)

Figure 58 – (a) An example of the pictures achieved for patient 16, and the analysed ROI positioning. (b) Mean values of the relative intensities versus the RTOG grade.

Patient 17

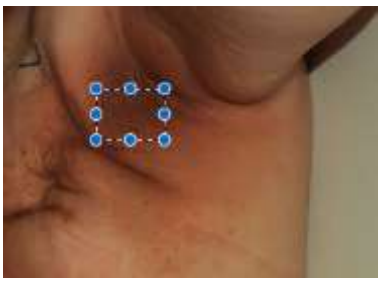

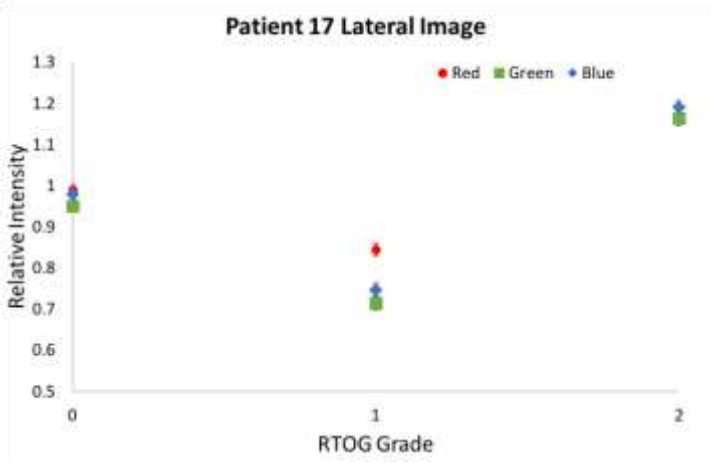

(a) (b)

Figure 59 – (a) An example of the pictures achieved for patient 17, and the analysed ROI positioning. (b) Mean values of the relative intensities versus the RTOG grade.

Patient 17 shows an interesting behaviour when the ROI has a grade 2. As seen before, for grade 0, the radio stays close to 1. To the grade 1, the ratio diminishes up to 0.9 for the red value and 0.8 for the green and blue value. As seen in *Figure 60*, the patient in the first medical return has an initial grade 2. Three weeks after, the complete ROI has a grade 2, were all the skin desquamates (*Figure 61).*

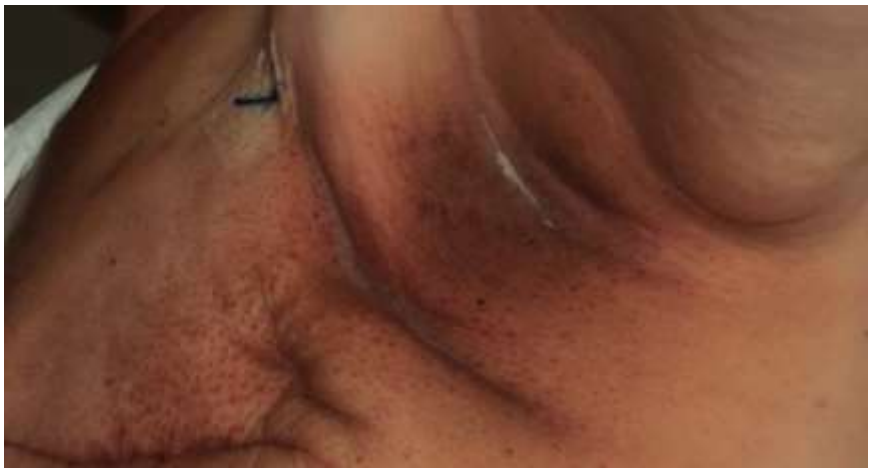

Figure 60 – Patient 17 grade 2 image in the first medical return, one week after finishing an hypofractionated treatment. The whole ROI is very red, but in the middle appears a little desquamation, which physicians already evaluates the region as a grade 2.

Figure 61 – Patient 17 grade 2 image in the second medical return, 4 weeks after finishing an hypofractionated treatment. The whole ROI desquamated, and in comparison with the normal skin outside the treatment area as it was in the beginning of the dose delivery, the skin is brighter.

Because of the full desquamation of the ROI in study, is that in the plot of *Figure 59b* that the ratio is above 1, because the whole ROI desquamated, and in comparison with the normal skin outside the treatment area as it was in the beginning of the dose delivery, the skin is brighter

Patient 18

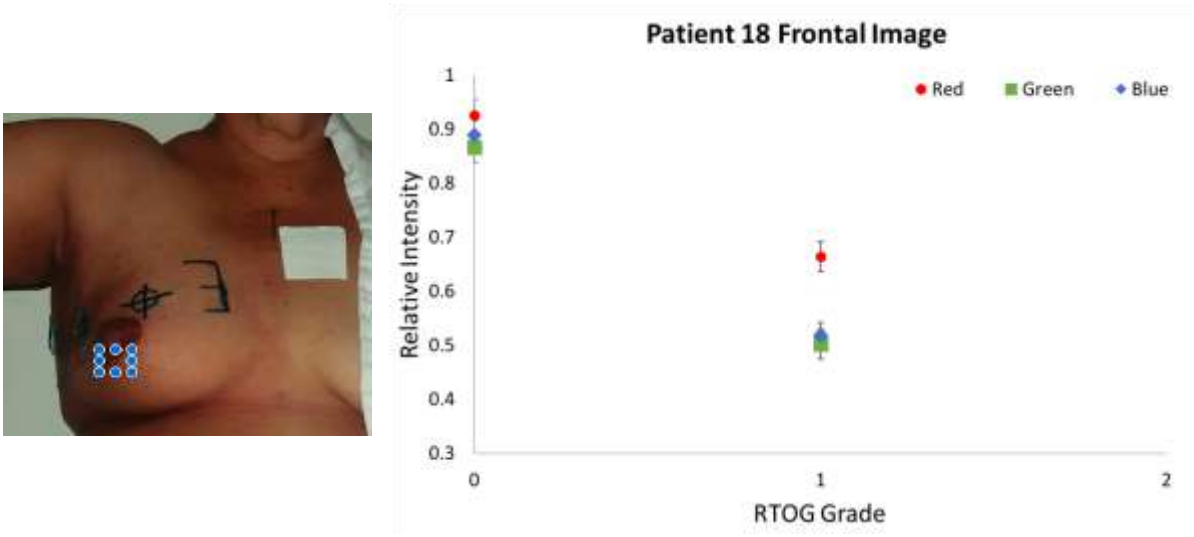

(a) (b)

Figure 62– (a) An example of the pictures achieved for patient 18, and the analysed ROI positioning. (b) Mean values of the relative intensities versus the RTOG grade.

Patient 18 has a grade 1 in both lateral and frontal image. Grade 0 values are almost the same, and for grade 1, the blue and green channel are close to 0.5, which as most of the time, the less sensitive channel is the red one.

(a) (b)

Figure 63 – (a) An example of the pictures achieved for patient 18, and the analysed ROI positioning. (b) Mean values of the relative intensities versus the RTOG grade.

Patient 19

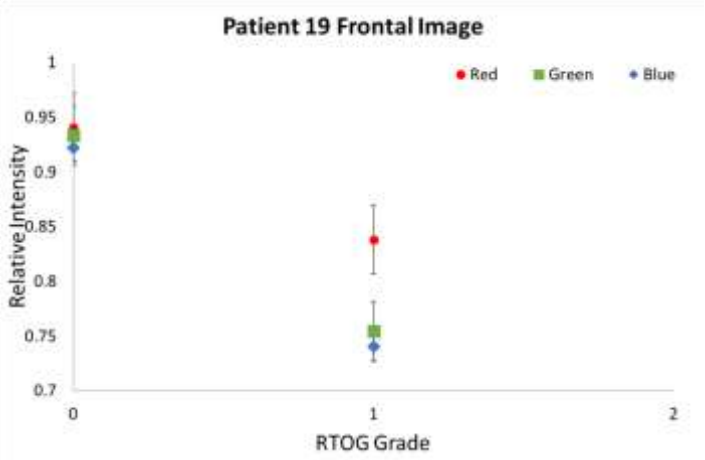

(a) (b)

Figure 64 – (a) An example of the pictures achieved for patient 19, and the analysed ROI positioning. (b) Mean values of the relative intensities versus the RTOG grade.

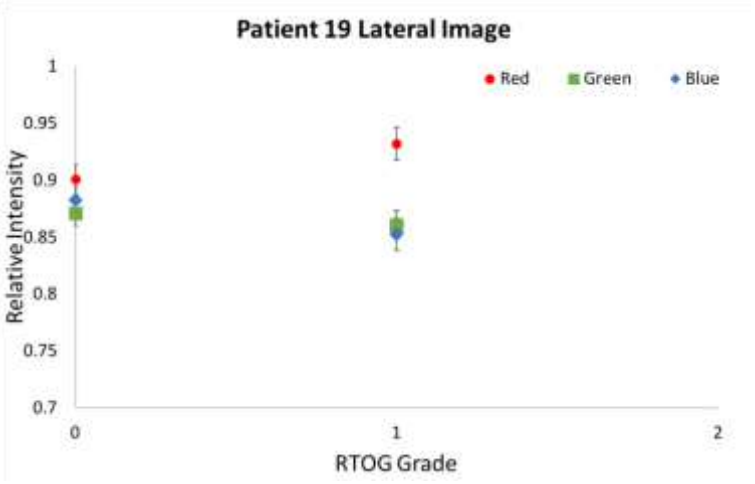

(a) (b)

Figure 65 – (a) An example of the pictures achieved for patient 19, and the analysed ROI positioning. (b) Mean values of the relative intensities versus the RTOG grade.

Patient 20

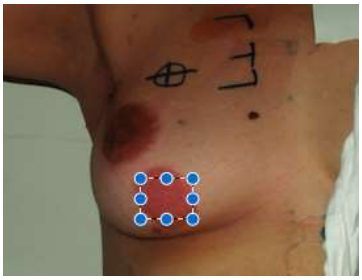

(a) (b)

Figure 66 – (a) An example of the pictures achieved for patient 20, and the analysed ROI positioning. (b) Mean values of the relative intensities versus the RTOG grade.

Patient 21

(a) (b)

Figure 67 – (a) An example of the pictures achieved for patient 21, and the analysed ROI positioning. (b) Mean values of the relative intensities versus the RTOG grade.

Patient 22

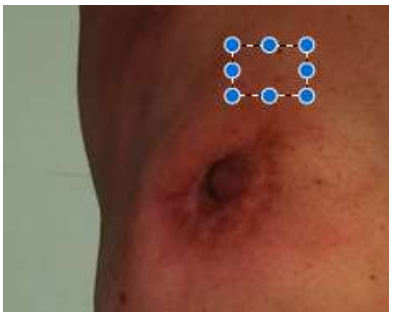

(a) (b)

Figure 68 – (a) An example of the pictures achieved for patient 22, and the analysed ROI positioning. (b) Mean values of the relative intensities versus the RTOG grade.

Patient 23

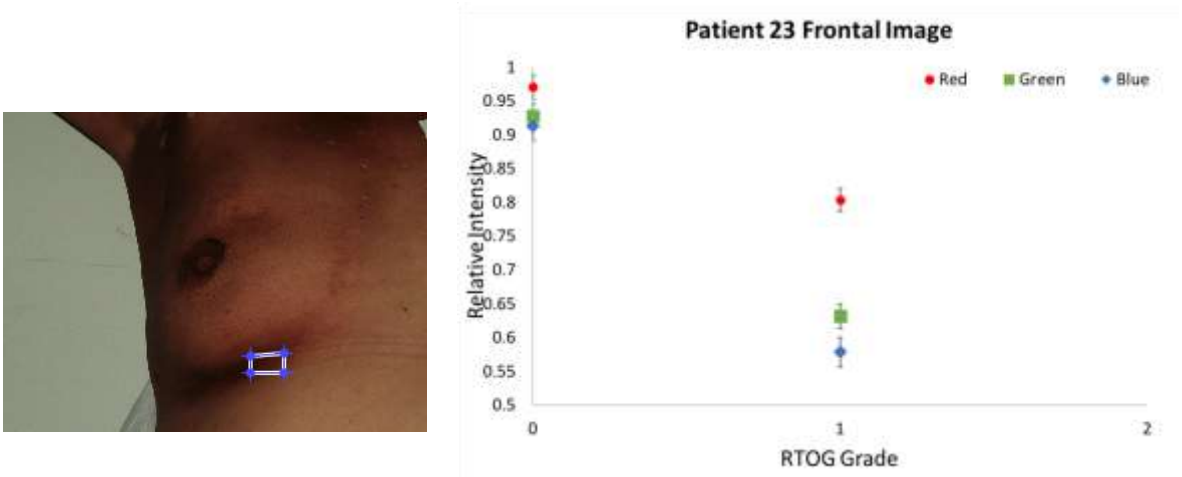

(a) (b)

Figure 69 – (a) An example of the pictures achieved for patient 23, and the analysed ROI positioning. (b) Mean values of the relative intensities versus the RTOG grade.

A table summarizing all this values is presented in the *Appendix D.*

For this first part of the results, in can be concluded that the channel G is the most sensitive to radiation dose and skin variations along the therapies. And, as the patient study group is so diverse in type of treatment, age and skin colour, that each patient has a different reaction to skin dose. Because of that, and in the try of finding a global response for all patients, that they will be divided in different groups as for example skin colour and treatment type to study the behaviour of the RGB colour, especially the green channel.

The patients were divided in skin groups: white, brown and dark, the mean of the normalized ratios of the lateral and frontal images, was calculated. For white skin, it was plotted the means versus the RTOG grade as seen in *Figure 70*. For grade 0, all values are close to 1, 0.96±0.04 for the Red channel, 0.94±0.04 for the Green channel, and 0.94±0.03 for the blue channel. For the grade 1 the variation in the channel R is minimum (0.93±0.05), but both Green and Blue goes to 0.85±0.04 and 0.84±0.04 respectively; and for grade 2, the R channel continue

almost constant (0.92±0.05), and the Green and Blue channel diminishes up to 0.77±0.05 and 0.80±0.04. This results insists us to think that the most sensitive channel is the Green one.

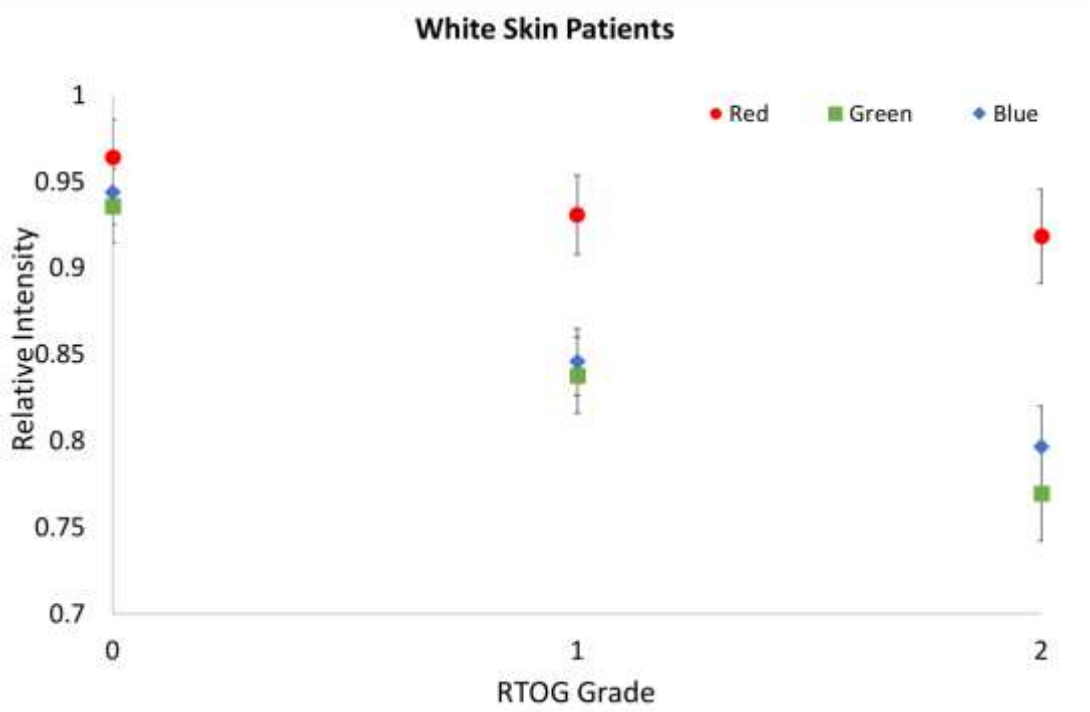

Figure 70 – Ratio mean for the RGB colour space vs the RTOG Grade for white skin.

For brown skin, as seen in *Figure 71*, in the grade 0, all values are close to 0.8, 0.81±0.05 for the Red channel, 0.81±0.04 for the Green channel and for the Blue channel, 0.80±0.04. In this case, in comparison with white skin patients, the ratio interval for grade 0 is bigger, showing that for even a RTOG grade 0, the skin has a considerable variation in intensity. For the grade 1 the variation in the channel R is 0.67±0.054, and the G and Blue decreases up to 0.60±0.04 and 0.57±0.04 respectively. For grade 2, we can see a different behaviour in comparison with white skin patients. The R channel rises to 0.79±0.04, the Green stays in 0.59±0.04, and Blue channel increases to 0.63±0.03. This occurs by the fact that in brown skins patients with grade 2, in the ROI that is being analysed for grade 0 and 1, appears a desquamation, leaving the skin more whiter, and it is more noticeable in brown skin patients.

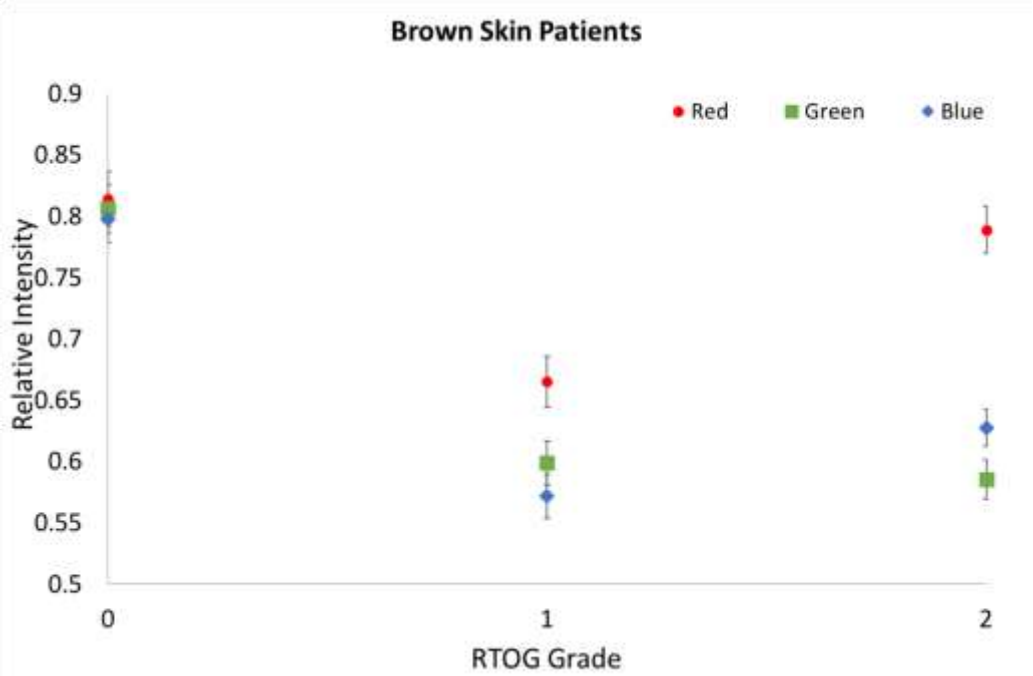

Figure 71 - Ratio mean for the RGB colour space vs the RTOG Grade for white skin.

For dark skin, as seen in *Figure 72*, in the grade 0, all values are similar to those in brown skin patients, 0.84±0.05 for the Red channel, 0.82±0.04 for the Green channel and for the Blue channel, 0.81±0.04.. For the grade 1 the variation in the channel R is 0.61±0.03, and the G and Blue decreases up to 0.53±0.03 and 0.50±0.03 respectively. For grade 2, we can see a different behaviour in comparison with white skin patients. The R channel is 0.54±0.02, the Green is 0.50±0.04, and Blue channel increases to 0.52±0.02. In this cases there is a trend to an increase in the ratio values for grade 2, but this can means that the desquamations that appeared in the ROI must be smaller, so the is not a considerable variation in the ratio value.

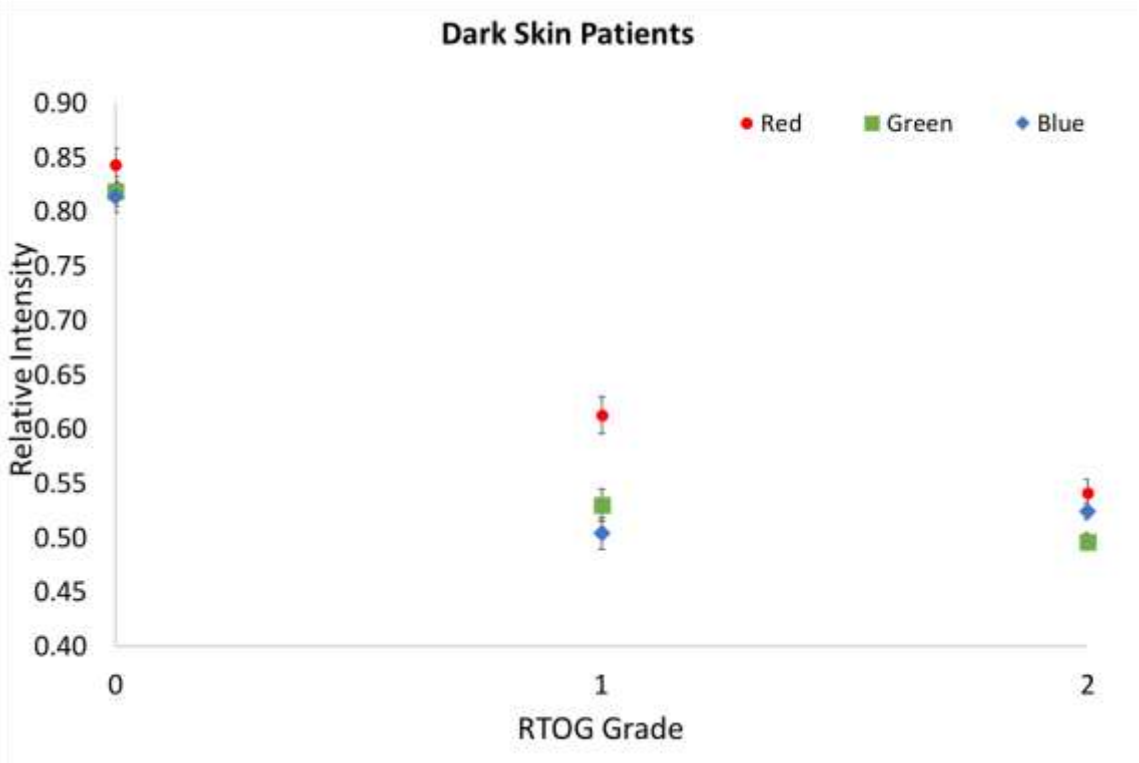

Figure 72 - Ratio mean for the RGB colour space vs the RTOG Grade for white skin.

For the comparison of this values, the *t*-test results are summarized in *Appendix E*, in the tables 10-18. First, comparisons for the same skin colour between the results of grade 0 and grade 1; and grade 1 and grade 2 for the three channels of the RGB channel were done. A significant difference was found between the mean normalized intensities of the grade 0 and grade 1for channel R in white skin ($p = 0.04$) and brown skin ($p = 0.02$); and between the mean normalized intensities of the grade 1 and grade 2 in brown skin ($p = 0.02$). For channel G between the mean normalized intensities of the grade 0 and grade 1 in white skin ($p = 0.004$) and brown skin ($p = 0.005$); and between the mean normalized intensities of the grade 1 and grade 2 in white skin ($p = 0.005$). For the blue channel, only between the mean normalized intensities of the grade 0 and grade 1 in white skin ($p = 0.004$), brown skin ($p = 0.002$) and dark skin ($p = 0.05$). The number of patients presenting grade 2 radiodermatitis and dark skin limited this study.

Another comparison was done between the results of the mean relative intensities for the same radiodermatitis with the combinations between the three skin colours and for all the RGB channels, summarized in the tables 19-27 of *Appendix E*.

By comparing the mean intensity values for the radiodermatitis grades achieved for the patients with white and brown skin, a significant difference was found for comparisons of grade 0 and grade 1 radiodermatitis grade for all the channels. For the grade 0 comparisons p-values of 1.10^{-3}, 0.01 and 0.01 were found for the red, green and blue channels respectively, while, for the grade 1 comparisons p-values of 2.10^{-6}, 3.10^{-4} and 6.10^{-5} were found for the red, green and blue channels respectively.

For the comparisons for white and dark skin a significant difference was found for comparisons of all grades of radiodermatitis for all the channels. For grade 0 comparisons, p-values of 2×10^{-4}, 1×10^{-3} and 0.01 were found for the red, green and blue channels respectively; for grade 1 comparisons p-values of 2×10^{-5}, 1×10^{-4} and 5×10^{-4} were found for the red, green and blue channels respectively, and, for grade 2 comparisons p-values of 0.002, 0.04 and 0.04 were found for the red, green and blue channels respectively.

Finally, for the comparisons of brown and dark skin a significant difference was found only for grade 2 radiodermatitis for the blue channel ($p = 0.04$).

These results indicate that the proposed methodology could not provide a single intensity value applied for all skin colours, since a significant difference between the relative intensities was found for the presented comparisons, except for the brown and dark skin that shows grade 2 radiodermatitis.

The comparison of the presented results with other published papers is not possible because no other study evaluated the radiodermatitis with this methodology.

Conclusions

This study demonstrated an approach to evaluate radiodermatitis quantitatively. Using normalized intensity ratios, it was obtained three different ratio intervals for each grade of radiodermatitis for each skin colour. For white, brown and dark skin colours significant difference between the normalized intensities was achieved depending on the grade. For white skin, a significant value was obtained differentiating grade 0 and 1 of radiodermatitis. For brown skin, significant value was obtained differentiating grade 0 and 1, and differentiating grade 1 and 2. For dark skin, no significant value was obtained due to the small number of patients. Although all channels presented the significant difference for evaluation of grade 0 and 1 radiodermatitis, the most sensitive channel of the RGB colour space was the green channel, so we recommend its intensity intervals to be used on the presented quantitative evaluation.

Our methodology was not able to create an unique methodology for radiodermatitis. This is concluded for our results, which shows a different behaviour depending on the skin colour. An alternative for an unique metric would be the separation of the melanin contribution in the image intensities, and a posterior re-analysis of the intensities.

Improvements could be done for new image acquisition. For example, a better positioning of the patients before the image could help in the reproducibility of the study. Using an immobilizer, the same the patients use in the treatment couch, would leave the patient in the same position every day. Thus, image registration would not be necessary. In our case, as it was a public hospital, the amount of patients being treated was considerable. Also, many patients could not stay after being irradiated because they lived in other cities and they wanted to go back home as soon as possible.

This novel work is a good starting point for the study of radiodermatitis of different skin colours and treatment types. In the future, ours results could be analysed using the methodology of past studies, as for example, the erythema index. Improving as much as possible this methodology could in the future be a powerful tool for radiodermatitis evaluation. The used of polarized light showed us the advantage of seeing what a physician would not see in a skin evaluation. This work can bring real benefits for radiation therapy patients.

Funding Sources

This study was financed in part by the *Coordenação de Aperfeiçonamento de Pessoal de Nível Superior – Brasil (CAPES)*- Finance Code 001.

Bibliography

[1] J. Nyström, P. Geladi, B. Lindholm-sethson, J. Larson, A. Svensk, and L. Franzén, "Objective measurement of radiation induced erythema by nonparametric hypothesis testing on indices from multivariate data," *Chemometrics and Intelligent Laboratory System* vol. 90, pp. 43–48, 2008.

[2] C. R. Baines, W. McGuiness, and G. A. O'Rourke, "An integrative review of skin assessment tools used to evaluate skin injury related to external beam radiation therapy," *J. Clin. Nurs.*, vol. 26, no. 7–8, pp. 1137–1144, 2017.

[3] S. L. Jacques, J. C. Ramella-Roman, and K. Lee, "Imaging skin pathology with polarized light," *J. Biomed. Opt.*, vol. 7, no. 3, p. 329, 2002.

[4] J. D. Cox and J. Stetz, "OF THE RADIATION THERAPY ONCOLOGY AND THE EUROPEAN TREATMENT GROUP AND," *Int. J. Radiation Oncology Bio. Phys.* vol. 31 no 5. January, 1995.

[5] G. Sánchez and J. Nova, "Confiabilidad y reproducibilidad de la escala de fototipos de Fitzpatrick antes y después de un ejercicio de estandarización clínica," *Revista Biomédica* pp. 544–550, 2008.

[6] J. D'Orazio, S. Jarrett, A. Amaro-Ortiz, and T. Scott, "UV radiation and the skin," *Int. J. Mol. Sci.*, vol. 14, no. 6, pp. 12222–12248, 2013.

[7] M. H. A. Fadzil, S. Member, D. Ihtatho, A. M. Affandi, and S. H. Hussein, "Objective Assessment of Psoriasis Erythema for PASI Scoring," pp. 4070–4073, 2008.

[8] A. Harila, "Assessment of Skin erythema by eye, laser Doppler flowmeter, spectroradiometer, two channel erythema meter and Minolta chroma meter" *Dermatology Res.* pp. 278–282, 1993.

[9] E. Sattler, J. Welzel, E. Sattler, R. Kästle, and J. Welzel, "Optical

coherence tomography in dermatology," *Journal of Biomedical Optics* vol 18, no. 6, 2013.

[10] S. Wong, A. Kaur, M. Back, K. M. Lee, S. Baggarley, and J. J. Lu, "An ultrasonographic evaluation of skin thickness in breast cancer patients after postmastectomy radiation therapy," *Radiat. Oncol.*, vol. 6, no. 1, p. 9, 2011.

[11] B. Querleux, "Magnetic resonance imaging and spectroscopy of skin and subcutis," *Journal of Cosmetic Dermatology* pp. 156–161, 2004.

[12] A. Raina, R. Hennessy, M. Rains, J. Allred, D. Diven, and M. K. Markey, "Objective Measurement of Erythema in Psoriasis using Digital Colour Photography with Colour Calibration," pp. 3333–3336, 2014.

[13] M. Setaro and A. Sparavigna, "Quantification of erythema using digital camera and computer-based colour image analysis: a multicentre study," pp. 84–88, 2002.

[14] U. Mattssona, M. Jontell, and J. Cassuto, "Digital image analysis (DIA) of colour changes in human sk exposed to standardized thermal injury and comparison with laser doppler measurements," *Computer Methods* vol. 50, pp. 31–42, 1996.

[15] Y. Wengström, C. Forsberg, I. Näslund, and J. Bergh, "Quantitative assessment of skin erythema due to radiotherapy - Evaluation of different measurements," *Radiother. Oncol.*, vol. 72, no. 2, pp. 191–197, 2004.

[16] P. M. Putora, L. Paulis, and L. Plasswilm, "Automated Erythema Quantification in Radiation Therapy - a Java Based Tool," *Applied Medical Information* vol. 26, no. 1, pp. 1–6, 2010.

[17] A. Bourouis, A. Zerdazi, M. Feham, and A. Bouchachia, "M-health: Skin disease analysis system using smartphone's camera," *Procedia Comput. Sci.*, vol. 19, pp. 1116–1120, 2013.

[18] H. Matsubara *et al.*, "Objective assessment in digital images of skin erythema caused by radiotherapy," *Med. Phys.*, vol. 42, no. 9, pp. 5568–

5577, 2015.

[19] F. Irccs, I. Nazionale, R. Therapy, and O. Group, “Correspondence Comment on “ Objective assessment in digital images of skin erythema.”

[20] A. Madooei *et al.*, “Hyperspectral image processing for detection and grading of skin erythema,” p. 1013322, 2017.

[21] R. C. Gonzalez, R. E. Woods, and P. Hall, *Digital Image Processing*. .

[22] E. Hecht, "Optics "*fifth edition 5. Pearson*, Global Edition. 2017

[23] E. K. Hansen, Handbook of Evidence-Based Radiation Oncology. 3rd Edition. Springer. USA 2018.

[24] Jiade J. LU,"Decision Making in Radiation Oncology" .*Medical Radiology Radiation Oncology*. Volume 1. Springer, Heidelberg, 2011.

[25] A. U. Schratter-Sehn, “Breast cancer radiotherapy,” *Hamdan Med. J.*, vol. 5, no. 1, pp. 529–536, 2012.

[26] K. S. Kim, K. H. Shin, N. Choi, and S. Lee, “Hypofractionated whole breast irradiation : new standard in early breast cancer after breast-conserving surgery,” *Radiation Oncology Journal* vol. 34, no. 2, pp. 81–87, 2016.

[27] T. Igarashi, K. Nishino, and S. K. Nayar, “The Appearance of Human Skin : A Survey,” vol. 3, no. 1, pp. 1–95, 2007.

[28] A. J. Kole, L. Kole, and M. S. Moran, “Acute radiation dermatitis in breast cancer patients: Challenges and solutions,” *Breast Cancer Targets Ther.*, vol. 9, pp. 313–323, 2017.

[29] G. Tortorelli *et al.*, “Standard or hypofractionated radiotherapy in the postoperative treatment of breast cancer: A retrospective analysis of acute skin toxicity and dose inhomogeneities,” *BMC Cancer*, vol. 13, 2013.

[30] A. Goshtasby, “PIECEWlSE LINEAR MAPPING FUNCTIONS FOR IMAGE REGISTRATION,” *Pattern Recognition* vol. 19, no. 6, pp. 459–466, 1986.

Appendix A

TERMO DE CONSENTIMENTO LIVRE E ESCLARECIDO

Você está sendo convidado a participar, como voluntário(a), da pesquisa intitulada "Quantificação de Radiodermite através de Processamento de Imagens", conduzida pelo pesquisador e mestrando em física aplicada à medicina e biologia da Universidade de São Paulo, Ignacio Agustín Verdugo Naranjo, e pela pesquisadora e professora doutora do departamento de física da Faculdade de Filosofia, Ciências e Letras da Universidade de São Paulo, Juliana Fernandes Pavoni.

Este estudo tem por objetivo desenvolver um método computadorizado para avaliar automaticamente a mudança na colouração da pele pelo tratamento de radioterapia, efeito chamado radiodermite. Atualmente, não existe um método automático de medida para avaliá-la. Esse estudo não traz benefícios diretos para os participantes, mas os progressos neste estudo podem levar a uma melhoria no acompanhamento dos pacientes submetidos a radioterapia.

Você foi selecionado(a) por se encaixar no critério de seleção para a pesquisa, que consiste em: ser paciente de radioterapia em tratamento de câncer de mama ou câncer de cabeça e pescoço e ter mais de 18 anos. Sua participação não é obrigatória. A qualquer momento você poderá desistir de participar e retirar o seu consentimento. Sua recusa, desistência ou retirada de consentimento não acarretará prejuízo a você. Também a qualquer momento você poderá esclarecer dúvidas a respeito desta pesquisa.

Nenhum procedimento invasivo será realizado com você e sua identidade será preservada na divulgação dos resultados desta pesquisa. Dessa forma, o risco previsível referente a essa pesquisa é mínimo. Você poderá se sentir constrangido ao ser fotografado, mas garantimos que apenas o pesquisador responsável por este trabalho será o fotógrafo e o foco da foto é apenas a região que está sendo tratada, qualquer região vizinha e não tratada, será coberta no momento da foto. A imagem será obtida com câmeras digitais dedicadas para a pesquisa (por exemplo, máquina fotográfica, webcam e/ou câmera integrada ao aparelho celular) sem necessidade de ter contato físico (Não há outro jeito de conseguir a imagem). As imagens adquiridas serão armazenadas por um período de 5 anos, após esse prazo, serão descartadas. O pesquisador responsável se compromete a tornar públicos nos meios acadêmicos e científicos os resultados obtidos de forma consolidada e sem qualquer identificação de indivíduos participantes. Os dados coletados serão registrados e posteriormente analisados, culminando em possíveis publicações de artigos científicos.

Seu acompanhamento médico durante a realização dessa pesquisa seguirá o protocolo habitual para o seu tratamento em radioterapia, não sendo necessária nenhuma mudança em decorrência da sua participação nesta pesquisa. No caso de despesas adicionais decorrentes desta pesquisa e não de seu tratamento médico, haverá ressarcimento dos custos envolvidos.A sua participação não é remunerada. Embora seja improvável a ocorrência de algum dano, deve-se informar que o participante de pesquisa têm direito a indenização conforme as leis vigentes no país, caso ocorra dano decorrente de participação na pesquisa.

Rubrica do participante Rubrica do pesquisador

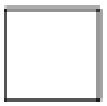

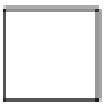

Sua participação nesta pesquisa consistirá em permitir que o pesquisador Ignacio Agustín Verdugo Naranjo (aluno estudante do mestrado em física aplicada à medicina e biologia) e quem fará entrega do TCLE, obtenha imagens exclusivamente da região de tratamento para serem analisadas através de programas de computador. A obtenção das imagens se dará diariamente ou duas vezes por semana no momento prévio ao tratamento diariamente ou durante sua avaliação pelo médico no Hospital das Clínicas de Ribeirão Preto, dessa forma nenhum deslocamento extra do paciente será necessário.

Caso você concorde em participar desta pesquisa, assine ao final deste documento, que possui duas vias, sendo uma delas sua, e a outra, do pesquisador responsável. Seguem os telefones e o endereço institucional do pesquisador responsável e do Comitê de Ética em Pesquisa – CEP, onde você poderá tirar suas dúvidas sobre questões éticas sobre o projeto e sua participação nele, agora ou a qualquer momento.

Ignacio Agustín Verdugo Naranjo. Telefone: (11) 98962-9696
Email: ignacioverdugo@usp.br

Prof. Dra. Juliana Fernandes Pavoni. Telefone: (16) 3315 0082
Email: jfpavoni@ffclrp.usp.br

Comitê de Ética em Pesquisa da Faculdade de Filosofia, Ciências e Letras de Ribeirão Preto - USP
Avenida Bandeirantes, 3900 - Bloco 01 - Prédio da Administração-SALA 07- 14040-901 - Ribeirão Preto - SP - Brasil
Fone: (16) 3315-4811
E-mail: coetp@ffclrp.usp.br

Eu, _____,
RG_____,considerando que recebi todos os esclarecimentos, que compreendi para que serve o estudo, que posso interromper a participação a qualquer momento sem justificar a minha decisão, que meu nome não sera divulgado, que não terei despesas e não receberei dinheiro, concordo em participar do estudo.

_____ _____
Nome do Voluntário(a) (impresso ou em letra de forma) Assinatura do Voluntário

Data: _____/____/_____ , Ribeirão Preto. Hora: _____

_____ _____
Nome da Testemunha (impresso ou em letra de forma) Assinatura da Testemunha

Data: _____/____/_____ , Ribeirão Preto. Hora: _____

Declaração do Pesquisador

Declaro que revisei este estudo e o termo de consentimento com o participante. Segundo meu entendimento, ele compreendeu os objetivos, os procedimentos, riscos e benefícios do estudo.

_____ _____
Nome do Pesquisador (impresso ou em letra de forma) Assinatura do Pesquisador

Data: _____/____/_____ , Ribeirão Preto. Hora: _____

Appendix B

Quantification of Radiodermatitis Through Image Processing: A Feasibility Study

Ignacio Verdugo-Naranjo, George Cunha Cardoso, Juliana Fernandes Pavoni

Physics Department, Faculty of Philosophy, Sciences and Letter of Ribeirão Preto, University of São Paulo, Ribeirão Preto, SP, Brazil.

1. Introduction

Radiotherapy is one approach used for the treatment of cancer. It uses ionizing radiation to eliminate or reduce cancer cells, the radiation is focalized to the tumour and the doses delivered to the healthy organs at risk around it are controlled, but it is impossible to not irradiate them. Among the tissues inevitably irradiated is the skin, which is the first layer of body tissue that can receive more or less doses of radiation accordingly to the type of treatment employed **[1]**, the damage to the skin is more pronounced when radiation interacts with irregular surfaces such as in the breast or the head and neck region. Some studies suggest that up to 95% of breast cancer patients treated with radiotherapy will experience some kind of cutaneous reaction **[1,2]**.

There are two types of skin side effects, acute and late. The acute effect has a visual appearance in which the skin begins to turn red throughout the treatment. This colour, better known as erythema, is caused by an increase in blood volume in the subpapillary vascular plexus **[3]**. The extent of erythema will depend on the dose, field size, fractionation and beam quality within an effort to diminish the damage to the skin **[2]**.

At present, the main tool used to assist the physician with this assessment is the one proposed by the Radiation Therapy Oncology Group (RTOG) and the European Organisation for Research and Treatment of Cancer (EORTC). In 1995, they presented a research-based method for the validation of skin assessment, which is a Scoring Schema for skin which goes from

grade 0 (no skin damage) to 4 (ulceration bleeding and necrosis), and where grade 5 relates to death of the patient associated to radiation late effects **[4]**. However, this evaluation is based on the visual evaluation and may be subject to inter-observer variability. Quantitative methods for this evaluation were presented such as optical assessments **[5,6,7]** and imaging-based assessments using ultrasound **[8,9]**, magnetic resonance **[10]** or digital colour photography **[11,12],** but all of them presents a limitation and the gold standard method to evaluate radiodermatitis is still the visual inspection.

This study aims to present a simple metric of the skin erythema evaluation by using digital colour photography acquired using polarized light for white and brown skin colours that could be used to help physicians to eliminate the subjectivity of the visual evaluation. The main advantage of this technique is the possibility of achieving information of the skin surface and underneath layers, which is possible because the propagation of light through biological tissues causes photon polarization changes due to scattering of tissues. This way, images with polarized light can select light that spreads back from the surface tissue, in contrast to the light that deepens into the fabric before final escape as diffuse reflectance and whose state of polarization has been completely randomized **[3]**. Thus, it is possible to distinguish this superficially retro-dispersed light from the fully reflected diffused light which is dominated by light penetrating deep into the dermis **[13]**.

2. Methodology

Patient Selection

After the approval of the Ethics Committee of the Faculty of Philosophy, Sciences and Letters of Ribeirão Preto, of the University of São Paulo, and the Ethical Committee of the Ribeirão Preto Medical School (HCFMRP-USP) (CAAE nº 73541017.20000.5407), 20 breast cancer patients over 18 years old that had undergone either conventional photon radiotherapy or hipofractionated photon radiotherapy were included in the study. The patients were treated five times a week to a total dose depending on the treatment with a total dose of 50 Gy in 25 fractions (2 Gy per fraction) for conventional treatment, and a total dose of 42.4 Gy in 16 fractions (2.65 Gy per fraction) **[14]**.

Patients of all pigmentary phototype were chosen to participate in the study. Also patients with non, partial or total mastectomy were included, as also, patients with all type of breast size. The patients were divided in two groups, white and brown skin. The group of white skin patient consists of 15 individuals with non, partial or total mastectomy. Patients undergoing both treatment types were considered. The group of brown skin had 5 individuals which undergone hypofractionated radiation therapy.

Camera and Polarizer

The camera used for image acquisition was a Casio EX-10, which possess a pixel number of 12.1 megapixels. Also, a right handed circular polarizer sheet was used in the image acquisition. It was located in front of the flash and the camera lens.

Image Acquisition

Follow-up of the patient's skin colour evolution was evaluated with photographs at the beginning of treatments (before being treated), throughout the treatment and one, and four weeks after finishing. Digital and polarized images were used in this study and their intensities in the RGB colour space was evaluated and correlated to the visual qualitative method using the RTOG schema.

Images were obtained for each patient in random days. So for example, for a hipo-fractionated breast cancer patient, images were obtained in the first and last day of treatment, in their medical return; and in different days along the treatments, as seen in *Figure 1*.

Figure 1 - Example of Image Acquisition for a hypo-fractionated patient.

The images were taken in a room without windows inside the radiotherapy service. Inside, they were seated in a wooden bench where they supported their backs on the wall. Their bench and the camera tripod were always located in the same place every day and for all the pictures Before each image, it was shown to the patient the image of the first day so they could repeat the same position of the arms. Even though this was done, many patients cause of their age, previous breast surgery and/or arm pain; weren't able to maintain the same positions for too many seconds. Also it is important to consider the differences in the images from one day to another cause of breath movement.

Digital photographs were taken from 2 different positions to reach all regions of the treatment field, frontal and lateral (*Figure 2*). For each position, a picture was taken without room light, and the camera flash was used. For the same image, it was taken with light circularly polarized orthogonally to a polarizer positioned on the camera lens.

Figure 2 - Example of the patient positioning for imaging acquisition.

All the images were analysed at the same time by two physicians to validate the grade of radiodermatitis using the RTOG scale and this classification was used to the presented numerical analysis.

Image Processing

All the images were processed using MatLab software, by a study of the intensity values of specific regions of interest (ROIs) in the RGB colour space along the treatment time.

As mentioned before, as the patients along their treatment weren't always able to maintain the same position and considering also their breath movement, the images along the treatment weren't always the same. To prevent errors in the processing, an image registration was done. Taking advantage of anatomical regions, skin marks and tattoos in the border of the treatment field on the patients, an image registration based on geometric transformation was done.

For each patient the reference points were chosen individually. The first of a set of images for a whole treatment was used as reference, so their points were named as *reference points.* For all the other images, the points were named as *moving points*. MatLab offers a function for doing the geometric transformation called "fitgeotrans" that moves the moving points to adjust them as close as possible to position of the corresponding reference points.

The function requires three reference points. So for example, for a lateral image of a hipo-fractionated patient, three references points were chosen in the border of the treatment field as seen on *Figure 3.*

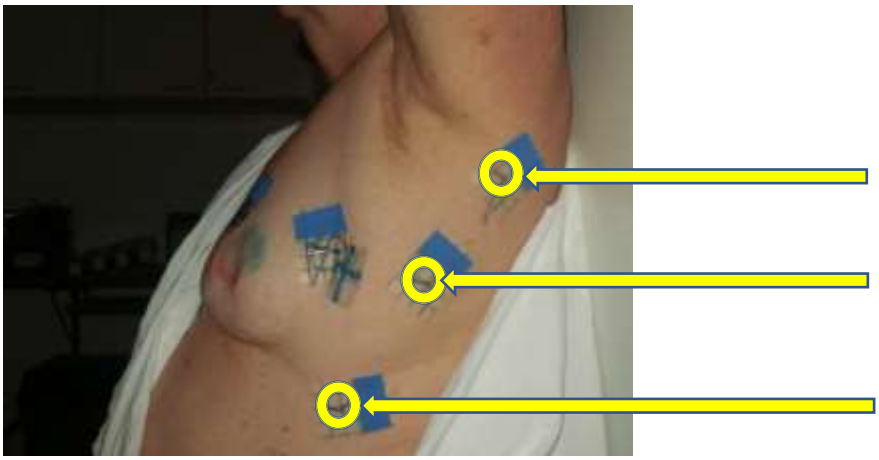

Figure 3 – Example of the three reference points selected in one image.

After the registration was done for all the images, it was chosen in any of them, mostly in the ones in the end of the treatment, a ROI were at least there was a grade 1 of radiodermatitis according to the RTOG scale. This assessment was done by any of the radiation therapists residents from the radiotherapy service.

This ROI was manually selected in the first image of the treatment in Matlab. Then, automatically the same ROI at the same position was selected in the registered images. For each ROI, it was calculated the mean of the pixel intensity in each channel in the space colour RGB . At the same time, this ROI was normalized by the mean intensity of a white stripe located outside the treatment area. This stripe was used in all the images for all the patients along their treatment (*Figure 4)*.

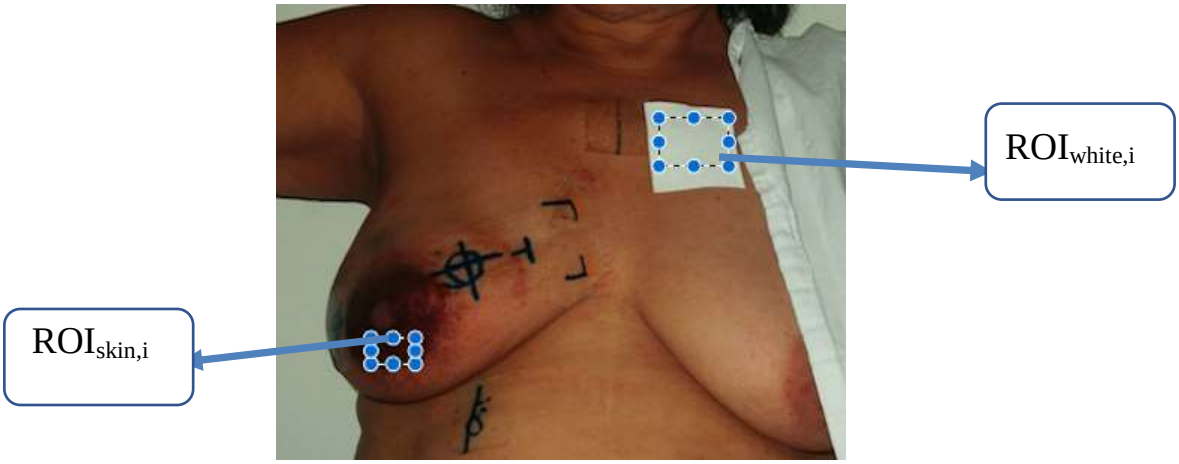

Figure 4 – Example of the positioning of the selected ROIs, one at the radiodermatitis and the other at the white stripe. The subscript *i* represent each channel of the RGB colour space

Normalizing by the white stripes helps in deleting differences in the flash camera intensity, because it is known that the light variates depending on the position. Also, as the camera was set in automatic mode, the illumination one day from another also variated.

To evaluate the significance of the difference between the mean values of intensity achieved for each radiodermatitis grade a statistical t-test analyses comparing the mean values of each radiodermatitis grade was performed. Outlier's values were excluded from the analyses.

3. Results and Discussion

The normalized intensities analysed for the white and brown skins are presented on table 1 and 2 respectively. For the white skin patients 15 presented radiodermatitis grade 0 and 1, and 5 presented radiodermatitis grade 2, while for the brown skin patients 5 presented radiodermatitis grade 0 and 1, and 1 presented radiodermatitis grade 2.

				Grade 0		Grade 1		Grade 2	
Patient	Treatment	Position	Channel	Mean normalized intensity	STD (s)	Mean normalized intensity	STD (s)	Mean normalized intensity	STD (s)
1	Hipofractionated	Lateral	R	1.01	0.04	0.82	0.05	-	-
			G	0.96	0.04	0.64	0.05	-	-
			B	0.96	0.03	0.63	0.04	-	-
2*	Conventional	Lateral	R	-	-	1.14	0.05	-	-
			G	-	-	1.20	0.05	-	-
			B	-	-	1.15	0.04	-	-
3	Hipofractionated	Frontal	R	0.99	0.05	1.01	0.04	-	-
			G	0.99	0.04	0.93	0.03	-	-
			B	0.98	0.03	0.93	0.03	-	-
4	Hipofractionated	Lateral	R	0.96	0.04	0.90	0.04	-	-
			G	1.03	0.04	0.94	0.04	-	-

			B	1.10	0.03	0.96	0.03	-	-
5	Hipofractionated	Frontal	R	1.05	0.04	0.93	0.03	-	-
			G	1.01	0.04	0.90	0.03	-	-
			B	1.02	0.03	0.87	0.03	-	-
6	Hipofractionated	Lateral	R	0.88	0.04	0.80	0.05	-	-
			G	0.80	0.03	0.65	0.03	-	-
			B	0.84	0.03	0.72	0.03	-	-
7	Hipofractionated	Frontal	R	0.82	0.06	0.48	0.05	-	-
			G	0.76	0.05	0.39	0.04	-	-
			B	0.76	0.05	0.38	0.05	-	-
8	Conventional	Frontal	R	0.91	0.06	0.83	0.06	0.90	0.06
			G	0.87	0.06	0.76	0.06	0.77	0.06
			B	0.89	0.05	0.76	0.05	0.78	0.05
9	Hipofractionated	Lateral	R	0.96	0.04	0.83	0.04	0.78	0.04
			G	0.92	0.06	0.68	0.06	0.59	0.06
			B	0.93	0.05	0.74	0.05	0.66	0.04
10	Hipofractionated	Lateral	R	0.86	0.04	0.71	0.03	-	-
			G	0.77	0.03	0.46	0.03	-	-
			B	0.77	0.03	0.50	0.03	-	-
11	Conventional	Frontal	R	0.99	0.03	1.02	0.06	0.84	0.06

			G	0.91	0.04	0.91	0.03	0.63	0.04
			B	0.93	0.03	0.94	0.04	0.61	0.03
12	Hipofractionated	Lateral	R	0.99	0.03	0.84	0.03	1.19	0.03
			G	0.95	0.03	0.71	0.03	1.16	0.04
			B	0.98	0.03	0.75	0.03	1.19	0.04
13	Hipofractionated	Lateral	R	0..91	0.03	-	-	-	-
			G	0.87	0.02	-	-	-	-
			B	0.88	0.02	-	-	-	-
14	Hipofractionated	Lateral	R	0.94	0.06	0.84	0.06	-	-
			G	0.93	0.06	0.75	0.06	-	-
			B	0.92	0.05	0.74	0.05	-	-
15	Hipofractionated	Lateral	R	0.99	0.02	1.15	0.06	-	-
			G	0.98	0.02	1.03	0.03	-	-
			B	0.98	0.02	0.99	0.03	-	-

Table 1 – Normalized intensities for the white skin patients achieved for each channel of the RGB colour map for each radiodermatitis grade.

				Grade 0		Grade 1		Grade 2	
Patient	Treatment	Position	Channel	Mean normalized intensity	STD	Mean normalized intensity	STD	Mean normalized intensity	STD
1	Hipofractionated	Lateral	R	0.88	0.04	0.89	0.05	-	-

			G	0.89	0.03	0.71	0.05	-	-
			B	0.88	0.02	0.71	0.04	-	-
2	Hipofractionated	Frontal	R	0.97	0.04	0.80	0.05	-	-
			G	0.93	0.04	0.63	0.03	-	-
			B	0.91	0.04	0.58	0.02	-	-
3	Hipofractionated	Lateral	R	0.81	0.05	0.72	0.05	0.20	0.06
			G	0.76	0.03	0.60	0.03	0.27	0.04
			B	0.76	0.02	0.61	0.02	0.25	0.03
4	Hipofractionated	Frontal	R	0.97	0.08	0.90	0.08	-	-
			G	0.93	0.08	0.71	0.08	-	-
			B	0.95	0.06	0.74	0.06	-	-
5	Hipofractionated	Frontal	R	0.82	0.02	0.48	0.02	-	-
			G	0.76	0.02	0.39	0.02	-	-
			B	0.76	0.02	0.38	0.02	-	-

Table 2 – Normalized intensities for the brown skin patients achieved for each channel of the RGB colour map for each radiodermatitis grade.

Table 3 presents the mean values of the normalized intensities for both skin colour evaluated and figure 5 presents the graphical comparison.

	White skin	Brown skin

Grade	Channel	Mean intensity values	STD (s)	Mean intensity values	STD (s)
0	R	0.95	0.04	0.89	0.04
	G	0.91	0.04	0.85	0.04
	B	0.92	0.04	0.85	0.03
1	R	0.92	0.05	0.76	0.05
	G	0.82	0.04	0.61	0.04
	B	0.83	0.04	0.61	0.03
2	R	0.89	0.04	0.20	0.06
	G	0.75	0.05	0.27	0.04
	B	0.78	0.04	0.25	0.03

Table 3 – Mean intervals of normalized intensities for the white and brown skins for each radiodermatitis grade achieved by the studied patients.

Figure 5 – Graphical comparisons of the normalized intensity as a function of the radiodermatitis grade.

It is possible to see that the normalized intensities decrease as the radiodermatitis grade increase and that the brown skin presents a more pronounced decrease. Considering the RGB colour space, the red channel is less sensitivity to this variation than the green and the blue ones. In addition, the responses of the green and blue channel are close for all evaluated radiodermatitis grades and this happened for both skin colours. These channels also presented the highest normalized intensity variation with the radiodermatitis grades.

For the white skin, if we analyse the mean values presented for each channel, a significant difference in the t-test was found between the mean normalized intensities of the grade 0 and grade 1 for all colour spaces ($p = 0.0209$; $p = 0.0033$ and $p= 0.0143$ for channels red, green and blue respectively). No significant difference was found between the normalized intensity ranges of the grade 1 and 2 ($p = 0.1407$; $p = 0.2630$ and $p= 0.2986$ for channels red, green and blue respectively), this is probably due to the small number of patients that presented a grade 2 radiodermatitis.

For the brown skin, the t-test was only applied to evaluate the significance of the difference between grade 0 and 1 radiodermatitis normalized intensities, grade 2 radiodermatitis was not evaluated because only one patient present it. No significant difference was found for the normalized intensities achieved for grade 0 and 1 for the red channel ($p = 0.1556$), but a significant difference was found for the green and blue channels ($p = 0.0085$ and $p= 0.0108$ for the green and blue colour channels).

The green channel was the most sensitivity channel for the evaluation of the radiodermatitis grade for both skin colours, being the ideal channel to be used in a quantitative evaluation of the radiodermatitis based on the normalized intensities of the images acquired along the treatment.

The use of the polarized images in this study was a try to eliminate the oiliness influence in the comparison of intensity values between different patients.

Even though past researches attempted similar ways of evaluating quantitatively the radiodermatitis grade, they all lack of number of patients, or of a more variated sample of patients. This work included 20 individuals who: (1) had two types of skin colour, (2) had undergo two different types of radiation therapy, and (3) had previous total or no total mastectomy.

4. Conclusions

The study demonstrated an approach to evaluate radiodermatitis quantitatively. Using normalized intensity ratios, it was obtained three different ratio intervals for each grade of radiodermatitis for each skin colour. For white and brown skin colours a significant difference between the normalized intensities was achieved differentiating grade 0 and 1 of radiodermatitis, the small number of patients presenting grade 2 radiodermatitis limited the definition of a range of intensities for its evaluation. Although all channels presented the significant difference for evaluation of grade 0 and 1 radiodermatitis, the most sensitive channel of the RGB colour space was the green channel, so we recommend its intensity intervals to be used on the presented quantitative evaluation.

Funding Sources

The CAPES, CNPq and FAPESP are recognised for their financial support.

Conflict of Interest Statement

The authors report no conflicts of interest in this work

Acknowledgments

We acknowledge Alexandre Faustino and Ana Carolina Hamamura physicians of the Ribeirão Preto Medical School Hospital and Clinics for the discussions about the classification of the radiodermatitis grades of the patients.

References

[1] Baines C.R., McGuiness W., O'Rourke G.A. 2016. "An integrative review of skin assessment tools used to evaluate skin injury related to external beam radiation therapy." *Journal of Clinical Nursing* 26 (June): 1137-1144.

[2] Nystrom J., Geladi P., Lindholm-Sethson B., Larson J., Svensk A.C., Franzen L. 2008. "Objective Measurements of Radiotherapy-Induced Erythema." *Skin Research and Technology* 10: 242-250.

[3] Jacques S.L. *et al* 2002. "Imaging Skin pathology with polarized light." *Journal of Biomedical Optics* 7, no. 3 (July): 329-340.

[4] Cox J.D. *et al* 1995. "Toxicity criteria of the radiation therapy oncology Group (RTOG) and The European organisation for research and treatment of cancer (EORTC)." *International Journal of Radiation Oncology Biology Physics* 31: 1341–1346.

[5] Ahmad Fadzil M.H., Ihtatho D., Mohd Affandi A., Hussein S. H., 2009 "Objective assessment of psoriasis erythema for PASI scoring." *J. Med. Eng. Technol*.. 33, no. 7: 516–24.

[6] Lahti A., Kopola H.,Harila A. 1993. "Assessment of skin erythema by eye, laser doppler flowmeter, spectroradiometer, two channel erythema meter, and Minolta chromameter." *Dermatological Res.:* 278– 282.

[7] Elke Sattler J.W., Kastle R., 2013. "Optical coherence tomography in dermatology," *J. Biomed. Opt.*, 18, no. 6.

[8] Wong S., Kaur A., Back M, Lee K.M. , Baggarley S., Lu J.J. 2011. “An ultrasonographic evaluation of skin thickness in breast cancer patients after postmastectomy radiation therapy.,” *Radiat. Oncol*. 6, no. 1: 9.

[9] Warszawski A., Röttinger E.M, Vogel R., Warszawski N.1998. “20 MHz ultrasonic imaging for quantitative assessment and documentation of early and late postradiation skin reactions in breast cancer patients,” *Radiother. Oncol.* 47, no. 3: 241– 247.

[10] Querleux B. 2004. “Magnetic resonance imaging and spectroscopy of skin and subcutis,” *J. Cosmet. Dermatol.* 3, no. 3: 156–161.

[11] Raina A., Hennessy R., Rains M., Allred J., Diven D., Markey M.K. 2015 “Objective measurement of erythema in psoriasis using digital colour photography with colour calibration,” *Ski. Res. Technol.* 7: 1–6.

[12] Setaro M., Sparavigna A., 2002. “Quantification of erythema using digital camera and computer-based colour image analysis: a multicentre study.,” *Skin Res. Technol.* 8, no. 2: 84–8.

[13] Jacques S.L. *et al* 2002 “Imaging Skin pathology with polarized light.” *Journal of Biomedical Optics* 7, no. 3: 329-340.

[14] Lu Jiade J, *et al* 2011. *Decision Making in Radiation Oncology*. Heidelberg, Germany: Springer.

Appendix C

Table 4 – Casio EX-10 Specifications

Pixel Number	12.1 megapixels
Image Sensor	1/1.7-inch high-speed CMOS(back illuminated type) Total Pixels：12.76 megapixels(/million)
Operating Speed	Shutter Release Time: Approx. 0.014 seconds
Lens	Construction: 11 lenses in 8 groups, including aspherical lens. F-number: F1.8 to F2.5 Focal Length: F=6.0 to 24.0mm
Shutter Type	CMOS electronic shutter and mechanical shutter Shutter Speed: ½ to 1/2000 second
Aperture	F1.8 to F8.0
ISO Sensitivity	Still Images: Auto/ISO80/ ISO100/ISO200/ ISO 400/ ISO 800/ ISO 3200/ ISO 6400/ ISO 12800 Still Images: HS Night Shot: Maximum ISO25600
Self-timer	0 seconds, 2 seconds, Triple Self-Timer
Built-in Flash	Flash Mode: Auto, Flash off, Flash on, Red Eye Reduction Flash Range: Approx. 0.8-10.9m

Table 5 – Circular Polarizer Sheet Specifications

Size	300mm x 300mm
Type	high contrast circular polarizer
Transmittance	single (42%) ; parallel (35%) ; crossed (0.5%)
Colour	neutral grey circular polarizer
Polarizing efficiency	99.98%
Retardation film	125nm
UV-Cut	Yes
Thickness	0.28mm
Durability	60°C / 90% RH / 500 Hours

Appendix D

*Table 6. Normalized intensities for the **White Skin** patients achieved for each channel of the RGB colour map for each radiodermatitis grade. MNI - Mean Normalized Intensity; σ - Standard Deviation.*

Patient Information				Grade 0		Grade 1		Grade 2	
Patient	**Treatment**	**Position**	**Channel**	**MNI**	**σ**	**MNI**	**σ**	**MNI**	**σ**
1	Hypofractionated	Lateral	R	1.01	0.04	0.82	0.05	-	-
			G	0.96	0.04	0.64	0.05	-	-
			B	0.96	0.03	0.63	0.04	-	-
	Hypofractionated	Frontal	R	1.00	0.02	1.07	0.02	-	-
			G	0.98	0.02	0.99	0.02	-	-
			B	0.99	0.02	1.01	0.02	-	-
2	Conventional	Lateral	R	-	-	1.14	0.05	-	-
			G	-	-	1.20	0.05	-	-
			B	-	-	1.15	0.04	-	-
3	Hypofractionated	Frontal	R	0.90	0.06	1.00	0.07	-	-
			G	0.84	0.08	0.89	0.08	-	-
			B	0.83	0.06	0.88	0.07	-	-
4	Hypofractionated	Lateral	R	1.00	0.02	0.93	0.02	-	-
			G	1.00	0.02	0.98	0.02	-	-
			B	0.99	0.02	1.00	0.02	-	-
	Hypofractionated	Frontal	R	0.99	0.05	1.01	0.04	-	-
			G	0.99	0.04	0.93	0.03	-	-
			B	0.98	0.03	0.93	0.03	-	-
5	Hypofractionated	Lateral	R	0.96	0.04	0.90	0.04	-	-
			G	1.03	0.04	0.94	0.04	-	-
			B	1.10	0.03	0.96	0.03	-	-
8	Hypofractionated	Frontal	R	1.05	0.04	0.93	0.03	-	-
			G	1.01	0.04	0.90	0.03	-	-
			B	1.02	0.03	0.87	0.03	-	-
10	Hypofractionated	Lateral	R	0.86	0.04	0.71	0.03	-	-
			G	0.77	0.03	0.47	0.03	-	-
			B	0.77	0.03	0.50	0.03	-	-
	Hypofractionated	Frontal	R	0.99	0.04	0.93	0.03	-	-

			G	1.01	0.03	0.83	0.03	-	-
			B	0.96	0.03	0.77	0.03	-	-
11	Hypofractionated	Frontal (mamilo)	R	0.99	0.06	0.97	0.06	0.93	0.06
			G	0.98	0.04	0.88	0.05	0.81	0.04
			B	1.02	0.04	0.93	0.04	0.87	0.04
	Hypofractionated	Frontal (mama)	R	0.95	0.08	0.96	0.08	0.86	0.08
			G	0.92	0.08	0.79	0.08	0.65	0.08
			B	0.94	0.06	0.84	0.06	0.66	0.06
13	Hypofractionated	Lateral	R	0.93	0.05	0.80	0.05	-	-
			G	0.84	0.06	0.62	0.06	-	-
			B	0.86	0.05	0.65	0.05	-	-
14	Conventional	Frontal	R	0.91	0.06	0.83	0.06	0.90	0.06
			G	0.87	0.06	0.76	0.06	0.77	0.06
			B	0.89	0.05	0.76	0.05	0.78	0.05
15	Hypofractionated	Lateral	R	0.96	0.04	0.83	0.04	0.78	0.04
			G	0.92	0.06	0.68	0.06	0.59	0.06
			B	0.93	0.05	0.74	0.05	0.66	0.04
	Conventional	Frontal	R	0.99	0.06	1.02	0.06	0.86	0.06
			G	0.91	0.06	0.91	0.06	0.63	0.06
			B	0.93	0.05	0.94	0.05	0.61	0.05
17	Hypofractionated	Lateral	R	0.99	0.03	0.84	0.03	1.19	0.03
			G	0.95	0.03	0.71	0.03	1.16	0.04
			B	0.98	0.03	0.75	0.03	1.19	0.03
19	Hypofractionated	Lateral	R	0.90	0.03	0.93	0.03	-	-
			G	0.87	0.02	0.86	0.02	-	-
			B	0.88	0.02	0.85	0.03	-	-
	Hypofractionated	Frontal	R	0.94	0.06	0.84	0.06	-	-
			G	0.93	0.06	0.75	0.06	-	-
			B	0.92	0.05	0.74	0.05	-	-
21	Hypofractionated	Lateral	R	0.99	0.02	1.15	0.06	-	-
			G	0.98	0.02	1.03	0.03	-	-
			B	0.98	0.02	0.99	0.03	-	-

*Table 7. Normalized intensities for the **Brown Skin** patients achieved for each channel of the RGB colour map for each radiodermatitis grade. MNI - Mean Normalized Intensity; σ - Standard Deviation.*

Patient Information				Grade 0		Grade 1		Grade 2	
Patient	**Treatment**	**Position**	**Channel**	**MNI**	**σ**	**MNI**	**σ**	**MNI**	**σ**
9	Hypofractionated	Lateral	R	0.88	0.04	0.80	0.05	0.75	0.05
			G	0.80	0.03	0.65	0.03	0.60	0.03
			B	0.84	0.03	0.72	0.03	0.65	0.03
	Hypofractionated	Frontal	R	1.01	0.04	1.02	0.03	-	-
			G	0.99	0.03	0.90	0.03	-	-
			B	0.97	0.03	0.86	0.03	-	-
12	Hypofractionated	Lateral	R	0.70	0.06	0.58	0.05	-	-
			G	0.65	0.05	0.52	0.04	-	-
			B	0.62	0.04	0.49	0.04	-	-
	Hypofractionated	Frontal	R	0.82	0.06	0.48	0.05	-	-
			G	0.76	0.05	0.39	0.04	-	-
			B	0.76	0.05	0.38	0.05	-	-
18	Hypofractionated	Lateral	R	0.93	0.02	0.66	0.02	-	-
			G	0.87	0.02	0.50	0.02	-	-
			B	0.89	0.02	0.52	0.02	-	-
	Hypofractionated	Frontal	R	0.45	0.06	0.39	0.06	-	-
			G	0.96	0.06	0.94	0.06	-	-
			B	0.95	0.05	0.79	0.05	-	-
20	Hypofractionated	Frontal	R	0.62	0.05	0.59	0.04	0.83	0.03
			G	0.37	0.04	0.32	0.04	0.57	0.03
			B	0.29	0.04	0.24	0.04	0.61	0.03
22	Hypofractionated	Frontal	R	0.95	0.05	0.66	0.04	-	-
			G	0.95	0.04	0.54	0.04	-	-
			B	0.95	0.04	0.56	0.04	-	-
23	Hypofractionated	Frontal	R	0.97	0.04	0.80	0.03	-	-
			G	0.93	0.04	0.63	0.04	-	-
			B	0.91	0.04	0.58	0.04	-	-

*Table 8. Normalized intensities for the **Dark Skin** patients achieved for each channel of the RGB colour map for each radiodermatitis grade. MNI - Mean Normalized Intensity; σ - Standard Deviation.*

Patient Information				Grade 0		Grade 1		Grade 2	
Patient	**Treatment**	**Position**	**Channel**	**MNI**	**σ**	**MNI**	**σ**	**MNI**	**σ**
6	Hypofractionated	Frontal	R	0.97	0.04	0.80	0.04	-	-
			G	0.93	0.04	0.63	0.04	-	-
			B	0.91	0.04	0.58	0.04	-	-
7	Hypofractionated	Frontal	R	1.03	0.04	0.92	0.05	-	-
			G	0.98	0.05	0.76	0.05	-	-
			B	0.99	0.04	0.76	0.04	-	-
16	Hypofractionated	Lateral	R	0.68	0.02	0.34	0.03	0.47	0.02
			G	0.69	0.02	0.34	0.02	0.45	0.02
			B	0.68	0.01	0.31	0.01	0.53	0.01
	Hypofractionated	Frontal	R	0.68	0.02	0.38	0.03	0.62	0.02
			G	0.69	0.02	0.39	0.02	0.55	0.02
			B	0.68	0.01	0.37	0.01	0.52	0.01

Table 9. Mean intervals of normalized intensities for the white, brown and dark skin patients for each radiodermatitis grade achieved by the studied patients. MIV – Mean Intensity Values; σ - Standard Deviation.

		White Skin		**Brown Skin**		**Dark Skin**	
Grade	**Channel**	**MIV**	**σ**	**MIV**	**σ**	**MIV**	**σ**
0	R	0.96	0.04	0.81	0.05	0.84	0.03
	G	0.94	0.04	0.81	0.04	0.82	0.03
	B	0.94	0.04	0.80	0.04	0.81	0.03
1	R	0.93	0.05	0.67	0.04	0.61	0.03
	G	0.84	0.04	0.60	0.04	0.53	0.03
	B	0.85	0.04	0.57	0.04	0.50	0.03
2	R	0.92	0.05	0.79	0.04	0.54	0.02
	G	0.77	0.05	0.59	0.03	0.50	0.02
	B	0.80	0.05	0.63	0.03	0.52	0.01

Appendix E

Comparison between results for the same skin colour

Table 10 – Comparison between different grades for white skin in the R channel

Channel R		White Skin	
		G1	G2
White Skin	G0	0.04	
	G1		0.06

Table 11 - Comparison between different grades for brown skin in the R channel

Channel R		Brown Skin	
		G1	G2
Brown Skin	G0	0.02	
	G1		0.02

Table 12 - Comparison between different grades for dark skin in the R channel

Channel R		Dark Skin	
		G1	G2
Dark Skin	G0	0.20	
	G1		0.89

Table 13 - Comparison between different grades for white skin in the G channel

Channel G		White Skin	
		G1	G2
	G0	0.004	
White Skin	G1		0.05

Table 14 - Comparison between different grades for brown skin in the G channel

Channel G		Brown Skin	
		G1	G2
	G0	0.005	
Brown Skin	G1		0.75

Table 15 - Comparison between different grades for dark skin in the G channel

Channel G		Dark Skin	
		G1	G2
	G0	0.06	
Dark Skin	G1		0.75

Table 16 - Comparison between different grades for white skin in the B channel

Channel B		White Skin	
		G1	G2
	G0	0.004	
White Skin	G1		0.08

Table 17 - Comparison between different grades for brown skin in the B channel

Channel B		Brown Skin	
		G1	G2
	G0	0.002	
Brown Skin	G1		0.47

Table 18 - Comparison between different grades for dark skin in the B channel

Channel B		Dark Skin	
		G1	G2
	G0	0.05	
Dark Skin	G1		0.67

Comparison between results for different skin colour

Table 19 - Comparison between brown and white skin for different grades for the R channel

Channel R		Brown Skin		
		G0	G1	G2
	G0	0.001		
	G1		0.00002	
White Skin	G2			0.277836276

Table 20 - Comparison between brown and white skin for different grades for the G channel

Channel G		Brown Skin		
		G0	G1	G2
	G0	0.01		
	G1		0.0004	
White Skin	G2			0.287488408

Table 21 - Comparison between brown and white skin for different grades for the B channel

Channel B				
		Brown Skin		
		G0	G1	G2
	G0	0.01		
	G1		0.00006	
White Skin	G2			0.2

Table 22 - Comparison between dark and white skin for different grades for the R channel

Channel R				
		Dark Skin		
		G0	G1	G2
	G0	0.0002		
	G1		0.00002	
White Skin	G2			0.002

Table 23 - Comparison between dark and white skin for different grades for the G channel

Channel G				
		Dark Skin		
		G0	G1	G2
	G0	0.001		
	G1		0.0001	
White Skin	G2			0.04

Table 24 - Comparison between dark and white skin for different grades for the B channel

Channel B				
		Dark Skin		
		G0	G1	G2
	G0	0.01		
	G1		0.0005	
White Skin	G2			0.04

Table 25 - Comparison between brown and dark skin for different grades for the R channel

Channel R				
		Dark Skin		
		G0	G1	G2
	G0	0.56		
	G1		0.23	
Brown Skin	G2			0.1

Table 26 - Comparison between brown and dark skin for different grades for the G channel

Channel G				
		Dark Skin		
		G0	G1	G2
	G0	0.38		
	G1		0.25	
Brown Skin	G2			0.21

Table 27 - Comparison between brown and dark skin for different grades for the B channel

Channel B				
		Dark Skin		
		G0	G1	G2
	G0	0.72		
	G1		0.377	
Brown Skin	G2			0.04